NTNU – Trondheim
Norwegian University of
Science and Technology

# Penetrating the Mucus Barrier

The Effect of Addition of Guluronate
Oligomers on the Mobility of Nanoparticles in
Porcine Small Intestinal Mucus

Solveig Lysfjord Sørensen

Biotechnology (5 year)
Submission date: May 2015
Supervisor: Kurt Ingar Draget, IBT
Co-supervisor: Catherine Taylor Nordgård, IBT

Norwegian University of Science and Technology
Department of Biotechnology

# Preface

This master thesis was conducted at the Norwegian Biopolymer Laboratory (NOBIPOL), Institute of Biotechnology at the Norwegian University of Science and Technology (NTNU) from September 2014 to May 2015. The thesis was written in collaboration with a research group led by Professor Kurt I. Draget, which is part of the COMPACT project.

The work with this thesis has been both interesting and challenging. I have learned a lot about the scientific working process, and I have become more experienced in working independently.

I would like to thank my supervisors for guidance and support throughout the work with the thesis. I would also like to thank Morten Johnsen Dille for guidance and help in the laboratory. My fellow students have been a valuable source for sharing both frustrations and successes. And last, but not least, I would like to thank my family and friends for motivation and moral support, and especially Halvor, without whom I could not have done this.

# Abstract

Oral delivery is the easiest and most used method of drug delivery. However, the gastrointestinal (GI) tract poses many hurdles for the drugs to overcome before they can reach their target. One of them is the viscous, adhesive, and constantly replenishing mucus layer. Mucus layer effectively hinders particles and microorganisms from passing through by several mechanisms: the steric, interactive, and dynamic barriers. Nanoparticle drug delivery systems can be modified to affect the solubility, stability, permeability or other properties of biopharmaceuticals, leading to improved bioavailability and an enhanced, controlled or more rapid therapeutic effect. Modification of nanoparticles in order to penetrate the mucus layer more efficiently is an attractive prospect to increase the efficacy of the drug. PEGylation is a technique for enhancing particle transport and mobility in mucus. Low molecular weight G-blocks have been shown to transiently weaken the mucus layer, possibly allowing for more rapid diffusion of substances.

In addition, biosimilar mucus is a proposed model for porcine small intestinal mucus (PSIM). Caco-2 cells, a common cell line used in drug absorption studies, are not compatible with native mucus. Biosimilar mucus could be an attractive alternative. It is necessary to assess the diffusion of large particles in biosimilar mucus in comparison with porcine small intestinal mucus, to evaluate the viability of the model.

In this study, the effect of PEGylation on nanoparticle mobility in PSIM and biosimilar mucus is examined. The effects of added G-blocks on the mobility of various types of nanoparticles in both PSIM and biosimilar mucus are studied. General nanoparticle mobility in biosimilar mucus and PSIM is compared. Nanoparticle mobility was measured using multiple particle tracking (MPT).

There was no consistent effect of adding G-blocks to increase particle mobility in porcine small intestinal mucus. This is in conflict with earlier reports. A possible explanation could be changes in mucus structure caused by repeated thawing and freezing. Biosimilar mucus, as it is today, was found to not be a suitable model for the transport of large entities like nanoparticles in porcine small intestinal mucus, because of the large differences in particle mobility observed between the two types of mucus. However, changes in the composition of biosimilar mucus could possibly produce a more viable model.

# Sammendrag

Oral levering er den enkleste og mest brukte metoden for levering av legemidler. Mage- og tarmkanalen stiller imidlertid mange hindringer som legemidler må overvinne før når sitt virkested i kroppen. En av dem er den viskøse, klebende og kontinuerlig nydannende slimlaget. Slimlaget i tarmen hindrer effektivt partikler og mikroorganismer fra å passere gjennom ved flere mekanismer: de steriske, interaktive og dynamiske barrierene. Medikamentleveringssystemer med nanopartikler kan endres for å påvirke oppløseligheten, stabiliteten, permeabilitet og andre egenskaper til legemidler, noe som fører til forbedret biotilgjengelighet og en mer effektiv, mer kontrollert eller raskere terapeutisk effekt. Modifikasjon av nanopartikler for å mer effektivt kunne penetrere slimlaget er et attraktivt prospekt for å øke effektiviteten av medikamenter. PEGylering er en teknikk for å øke partikkeltransport og mobilitet i slim. G-blokker med lav molekylvekt har vist seg å midlertidig svekke slimlaget, noe som muligens gjør at stoffer kan diffundere raskere gjennom slimet.

I tillegg er biosimilar-slim en foreslått modell for tynntarmsslim fra gris (PSIM). Caco-2-celler, en cellelinje som vanlig brukes i medikamentabsorpsjonsstudier, er ikke kompatible med naturlig slim. Biosimilar-slim kan være et attraktivt alternativ. Det er nødvendig å vurdere diffusjonen av store partikler i biosimilar-slim sammenlignet med PSIM, for å vurdere gyldigheten av modellen.

I denne studien undersøkes effekten av PEGylering på nanopartikkelmobilitet i PSIM og biosimilar-slim. Effekten av tilsatte G-blokker på mobiliteten til ulike typer av nanopartikler i både PSIM og biosimilar-slim er studert. Generell nanopartikkelmobilitet i biosimilar-slim og PSIM sammenlignes. Mobiliteten av fluorescente nanopartikler ble målt ved bruk av multiple particle tracking (MPT).

Samlet sett viser resultatene ingen konsekvent effekt av tilsetningen av G-blokker med lav molekylvekt på mobiliteten av nanopartikler i PSIM eller biosimilar-slim. En mulig forklaring kan være at slimstrukturen har blitt endret på grunn av repetert tining og frysing av slimet. Biosimilar-slim, slik det foreligger i dag, synes ikke å være en god modell for mobiliteten av større partikler, som nanopartikler, i PSIM. Det er mulig at endringer i sammensetningen av biosimilar-slim kan gi en mer gyldig modell.

# Abbreviations

| Abbreviation | Meaning |
|---|---|
| BSA | Bovine serum albumin |
| CF | Cystic fibrosis |
| CLSM | Confocal laser scanning microscope |
| COMPACT | Collaboration on the Optimization of Macromolecular Pharmaceutical Access to Cellular Targets |
| Da | Dalton |
| $DP_n$ | Degree of polymerisation |
| EDC | 1-Ethyl-3-(3-dimethylaminopropyl)carbodiimide hydrochloride |
| EDTA | Ethylenediaminetetraacetic acid |
| G | α-L-Guluronic acid |
| G-blocks | α-L-Guluronate oligomers |
| GI | Gastrointestinal |
| HBS | HEPES buffered saline |
| HEPES | 4-(2-Hydroxyethyl)piperazine-1-ethanesulfonic acid |
| M | β-D-Mannuronic acid |
| mPEGa | Methoxy-polyethylene glycol-amine |
| MPT | Multiple particle tracking |
| ms | Milliseconds |
| MSD | Mean square displacement |
| NDDS | Nanoparticle drug delivery systems |
| PC | Phosphatidylcholine |
| PEG | Polyethylene glycol |
| PG | Porcine gastric |
| PIM | Porcine intestinal mucus |
| PSIM | Porcine small intestinal mucus |
| Sulfo-NHS | N-Hydroxysulfosuccinimide |
| τ | Time scale |

# Table of contents

# 1. Background

## 1.1 The mucosal surfaces and drug delivery

Drugs can be delivered by a variety of methods. Drug delivery by intravenous (IV) or intramuscular (IM) therapy is effective and fast, but inconvenient because it requires trained personnel and medical equipment. This problem especially applies to individuals receiving treatment that require frequent doses of medicine. A much simpler alternative would be to administer the drug orally or via the lungs, as this would enable the patient to take the medicine without trained personnel and medical equipment. Oral delivery is the easiest and most used method of drug delivery. However, the gastrointestinal (GI) tract poses many hurdles for the drugs to overcome before they can reach their target. One of them is the viscous, adhesive, and constantly replenishing mucus layer.

The lungs and the GI tract are part of the mucosal surfaces of the body, as are the nose and the eye. The mucosal surfaces are covered in mucus, which is a natural barrier that has evolved to hinder viruses, bacteria and particulate matter from entering the body. The thickness of the mucus layer is dependent on its location (Ensign *et al.*, 2012). In the GI tract, the thickness has been reported as 50–600 µm in the stomach and 15–450 µm in intestine and colon (Norris *et al.* 1998, Khanvilkar *et al.* 2001). The thickest layers of gastrointestinal mucus are reported to be in the stomach and the colon (Lichtenberger 1995). Mucosal delivery of drugs, particularly large hydrophobic molecules, biologicals and delivery vehicles is hampered by drug entrapment in mucus followed by rapid clearance (Lai *et al.* 2009a). If one could temporarily weaken the mucus barrier to allow the drugs through, the problem with mucosal delivery of drugs would be circumvented. Permanently disabling or weakening the mucus barrier is not desired, as this would leave the patient vulnerable to infections. For example, Ensign *et al.* reports that "a 30 % depletion of mucus by pilocarpine in an *ex vivo* rat intestinal model led to a 3-fold increase in *E. coli* translocation" (Ensign *et al.* 2012).

## 1.2 Mucus

### 1.2.1 The composition and properties of mucus

Mucus is a water-based, complex and heterogeneous gel whose composition varies between both species, individuals and tissue. The mucus barrier is comprised of a secreted mucus layer and membrane-bound mucins on the surface of the cells, called the glycocalyx, which together form the mucosal surface. The secreted mucus layer is a mucin-based gel, where the mucin fibres are cross-linked and intertwined with each other. Mucins are the most important compounds for the gel formation of mucus (Sellers *et al.* 1988), even though they make up only 5 % or less of the mucus composition (Celli *et al.* 2005). The other 95 % are mostly water. The secreted and membrane-bound mucins share some common features, but only the secreted mucins take part in gel formation (Strous and Dekker 1992).

Mucins are a diverse family of glycoproteins in the MUC gene family, and so far, at least 21 MUC genes have been described (HUGO Gene Nomenclature Committee). They have an overall high molecular weight, which can range from 0.5 to 40 MDa (Lai *et al.* 2009a, Cu and Saltzman 2009, Thornton and Sheehan 2004). Mucins have a protein backbone that can be "naked" and hydrophobic in some regions, or be heavily glycosylated by oligosaccharides of varying size and grade of branching in other regions (Ensign *et al.* 2012). The various types of mucins differ by the protein backbone (Rose and Voynow 2006), but there are some similarities. One of these are the PTS regions, which are regions with repeated residues of the amino acids proline, threonine and serine. The PTS regions come in various lengths and amounts depending on the specific MUC gene the mucin originated from, and some regions have been reported to be 5000 amino acids long (Cone

2009). In general, the PTS regions make up about 20 to 55 % of the total composition of amino acids in the backbone (Van Klinken *et al.* 1995).

The threonine and serine amino acid residues in the protein backbone contain hydroxyl groups, on which the glycan side chains are bound through O-glycosylation linkages. The glycans are hydrophilic and contain about 1-20 monomers (Yang *et al.* 2012). Some common monomers in the glycans are N-acetylgalactosamine, N-acetylglucosamine, fucose, galactose, sialic acid and mannose (Bansil and Turner 2006, Thornton and Sheehan 2004). The glycosylation of the protein backbone gives the mucins a negative charge on average because of the sulphate and carboxylate groups of the monomers in the glycan side chains (Lichtenberger 1995). The carbohydrate side chains of the mucins drastically increase their molecular weight, and can comprise as much as 80 % of the mucin molecular weight (Kornfeld and Kornfeld 1976). The glycan side chains and the intra- and intermucin repulsion caused by their negative charges also increase the persistence length of the mucins (Cone 2009, Shogren *et al.* 1989), which is a parameter quantifying the stiffness of a polymer. An increase in persistence length corresponds to a less flexible and more rigid polymer structure.

The mucins are on average heavily glycosylated, but in between are hydrophobic regions with no glycosylation, often termed as “naked” regions (Cone 2009, Lai *et al.* 2009a). The hydrophobic regions contain many cysteine amino acid residues, about 10 % (Bansil and Turner 2006), and the disulphide bonds formed between the cysteine contribute to the more globular shape of these regions (Cone 2005, Lai *et al.* 2009b). Disulphide bonds can also crosslink different mucins together, causing polymerisation of mucins (Cone 2009). The cysteine rich regions are often found at the terminal ends of the mucin molecules, and large networks of mucins can therefore be formed by this crosslinking (Sheehan *et al.* 2004). These networks are not permanent, as the many different interactions between and within mucus components are constantly shifting. This alternating of hydrophilic and negatively charged glycosylated regions and hydrophobic cysteine-rich regions along the mucins gives rise to a heterogeneous charge profile, and many possible interaction sites with other mucins or mucus components. Cu and Saltzman report that each mucin molecule intersects from about 10 to 100 times with other mucins (Cu and Saltzman 2009). Figure 1.2.1.1 shows a schematic drawing of mucin structure, with the core protein and oligosaccharide side chains, in addition to possible interaction sites. These interactions can occur both within or between mucins, or between mucins and other components of mucus.

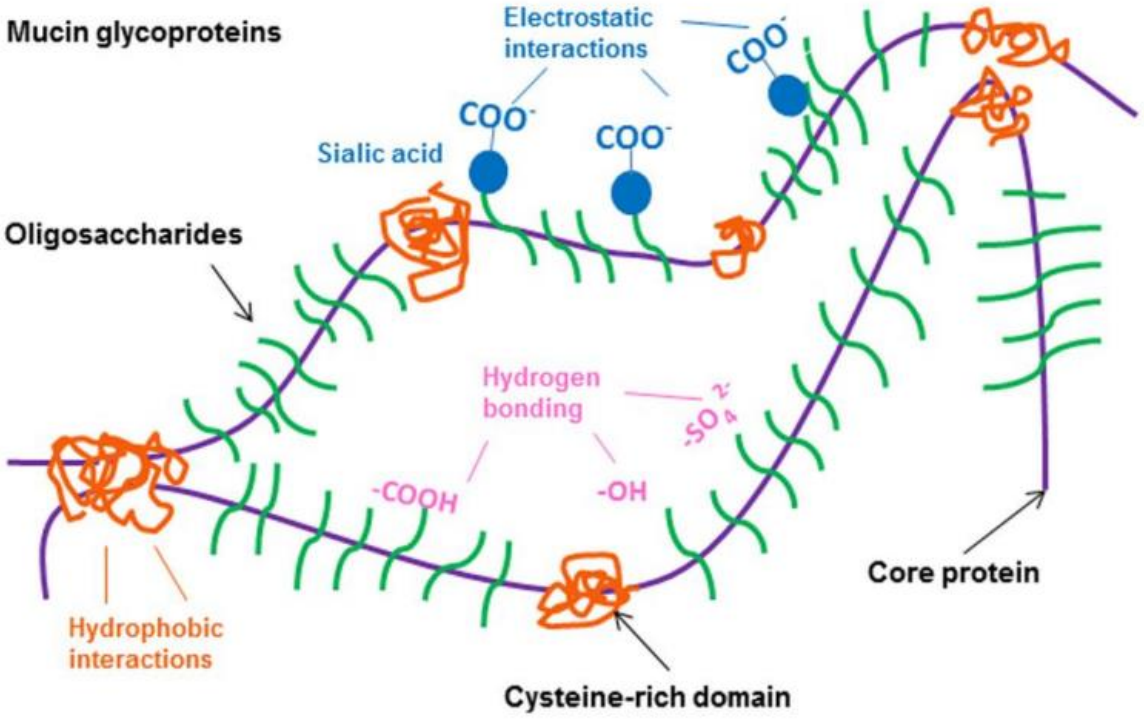


*Figure 1.2.1.1. Schematic drawing of mucins, including interaction sites for hydrogen bonding and electrostatic and hydrophobic interactions (Yang et al. 2012).*

Mucus also contains various other compounds besides mucins. Khanvilkar *et al.* reports that about 95 % of mucus is comprised of water (Khanvilkar *et al.* 2001), in addition to ions like $Na^+$ , $K^+$ , $Ca^{2+}$ and $Cl^-$. A layer of lipids is formed on the outward-facing side of the mucus layer. The lipids protect the mucus against free radicals and add to the selectivity of the mucus barrier (Cone 2005). The lipid layer also inhibits gases and hydrophobic compounds from crossing through the surface of the mucus layer (Cone 2009). The most important lipids are various free fatty acids and phospholipids, in addition to cholesterol (Bansil and Turner 2006). Various proteins like hormones, lysozymes, immunoglobulins and others are also part of the mucus composition (Cone 2005).

Finally, mucus contains various microorganisms, especially in the GI tract but also in the oral and nasal cavity and in the vaginal tract (Cone 2005). These microorganisms are generally not harmful and can even be helpful in digestion of some compounds, and in the inhibition of other, potentially harmful microorganisms (Savage 2005).

The interactions of the mucus components to form a gel are not fully understood. As mentioned, the mucins are thought to be the major contributors to the structure of the mucus gel. The mucins, with their glycan side chains and hydrophobic regions, form a network through various interactions like electrostatic and hydrophobic interactions, hydrogen bonds and van der Waals interactions. These interactions are not static, but rather shift and flicker over time (Kočevar-Nared *et al.* 1997, Cone 2009). A degree of mucin entanglement is also necessary for gel formation (Thornton and Sheehan 2004).

The structure of mucus, as described above, gives rise to some important properties of mucus; it is shear thinning, viscoelastic, and forms a selective barrier. That mucus is shear thinning means that its viscosity decreases with increasing shear rate (Smidsrød and Moe 2008). The shear thinning properties of mucus gives rise to a slippage plane as the entangled mucins are pulled apart (Cone

2009) when the mucus is subjected to shearing, as shown in Figure 1.2.1.2. The figure shows mucus in the GI tract, with a layer of firmly adherent mucus closest to the cells, and a layer of loosely adherent mucus further out. A slippage plane forms between the two layers, allowing transport of food through the intestines without damaging the epithelial cells (Ensign *et al.* 2012). This makes mucus an excellent lubricant, and demonstrates that mucins are forming a network through low affinity bonds and weak interactions. Linkages between the mucins are being continuously broken and reformed, allowing the mucus to maintain its structure even when put under stress (Cu and Saltzman 2009). These flickering weak interactions and bonds also contribute to the adhesive property of mucus, meaning that mucus sticks to surfaces and particles (Cone 2005, Bansil and Turner 2006).

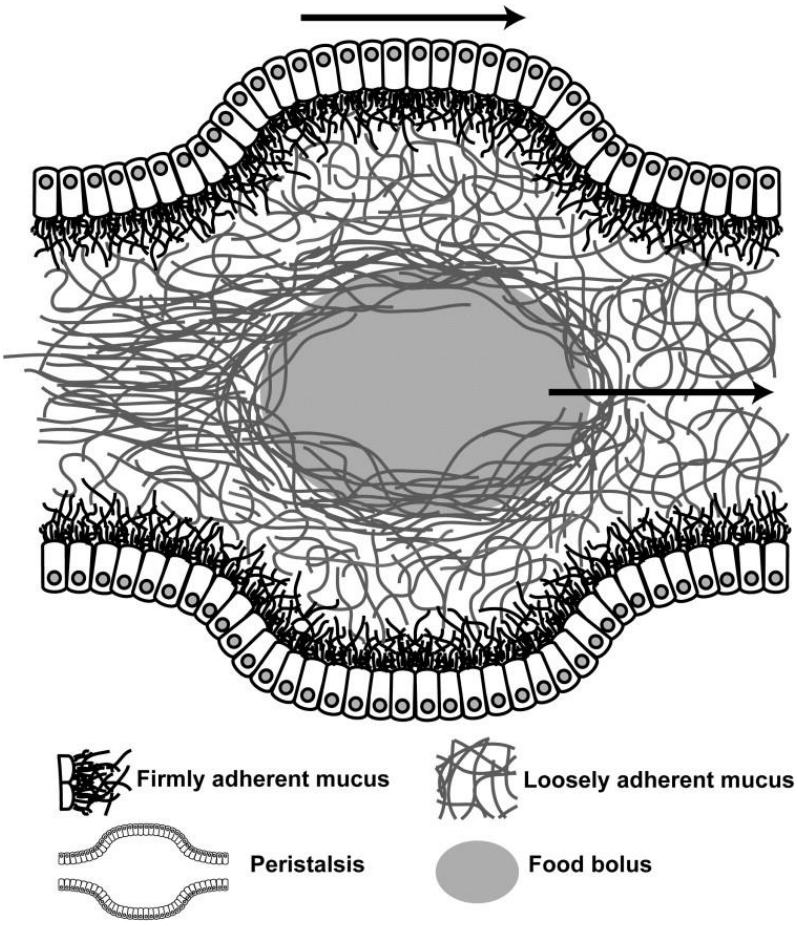


*Figure 1.2.1.2: Illustration of the organisation of the mucus layer in the GI tract, including the slippage plane formed between firmly and loosely adherent mucus that allows mucus to act as an excellent lubricant (Ensign et al. 2012).*

Exhibiting viscoelastic properties means that the substance is both viscous and elastic at the same time. Viscosity is a measure of the resistance of a fluid to deformation when subjected to shear stress. In common terms, more and less viscous fluids are often described as thick and thin. Elasticity is the property of a solid to return to its original state after being deformed by an outside force. Applying a small force to a mucus gel will cause it to deform as the interactions within and between mucus components shift, and when the force is removed, the mucus will regain some degree of its original form (Cone 2009). Since mucus is viscoelastic, it exhibits the properties of both a liquid and solid substance. The mucin content of the mucus gel is the most important factor for the viscoelastic properties, but the other components of mucus like water, ions and lipids also contribute (Ensign *et*

*al.* 2012). Viscoelastic properties are often measured and assessed by rheological methods, which measure the deformation of a substance in response to an applied force.

Mucus effectively hinders particles and microorganisms from passing through by several mechanisms: the steric, interactive and dynamic barriers (Sanders *et al.* 2009). Firstly, the mucins interact with each other as mentioned above and form a matrix that physically stops particles from moving through the mucus. This is the steric barrier. This barrier will obstruct particles that are above a certain size, depending on the mucus pore size, while smaller particles can in theory move through the pores. The pore size of mucus can vary between or within samples, as factors like the degree of glycosylation, electrostatic repulsion or attraction, and the extent of hydrophobic interactions and disulphide bonds can influence the structure of the mucins, and thereby the pore size. Pore size can be used as a measure of the degree of steric hindrance and can span over a large range. This is demonstrated by records of pore sizes in porcine tracheobronchial mucus measured to vary between 80 and 1500 nm, using PEGylated nanoparticles and atomic force microscopy (Yang *et al.* 2012).

Secondly, the mucins and other mucus components associate with the particle, forming multiple non-covalent interactions and trapping the particle in place. Although each individual bond or interaction may be weak, the number of interactions from the mucus to each particle adds up to a significant force (Cone 2009). As mentioned, the mucins are capable of hydrogen bonding and electrostatic interactions through the glycan side chains, and hydrophobic interactions through naked regions exposing the core protein, in addition to van der Waals interactions (Khanvilkar *et al.* 2001, Woodley 2001). All of these possible interaction sites gives mucus the attribute of being able to adhere to particles or microorganisms with a range of properties, like a hydrophobic surface or positive or negative charges (Yang *et al.* 2012).

Thirdly, new mucus is constantly produced and secreted from specialized cells, and the rapid turnover removes the trapped particles. This is the dynamic barrier, which hinders particles or microorganisms from reaching the underlying cells to potentially enter the body, unless they are able to rapidly penetrate the mucus layer. Most of the secreted mucus is digested and the components are recycled, but some are lost for example in faeces (Kwon *et al.* 2013). The mucus shedding and replenishment is especially high in the GI tract (Cone 2009), and an average human produces about 10 litres of mucus every day (Ensign *et al.* 2012).

### 1.2.2 Different mucus models

When conducting a drug absorption study different mucus models are available. This can pose a challenge in trying to compare studies of particle or compound mobility in mucus, because of the variety of mucus models being used. As mentioned, mucus layers can be found several places in the body. It poses a barrier for the entry of drugs into the body through delivery methods like oral, rectal, vaginal, nasal, or delivery to the lungs, as they are all part of the mucosal surfaces. Some of the mucus models in use are pig gastric mucin (purified or unpurified), and several types of artificial mucus, which are often reconstituted pig gastric mucus. Natural mucus is frequently used, like pig gastric or intestinal mucus, horse respiratory mucus, human cervicovaginal mucus, human airway mucus, and also natural mucus from diseased individuals like cystic fibrosis mucus or sputum. In addition, there are several *in vitro* models involving different cell lines, and *in vivo* models with rats or mice (Groo and Lagarce 2014).

Porcine gastric or intestinal mucins and mucus are often used for absorption studies simulating oral administration because of their resemblance to the mucus found in humans, for example regarding viscoelastic properties, structure and molecular weight (Sellers *et al.* 1991, Kararli 1995, Lai *et al.*

2009b). Some of the gene sequences for mucins in pigs have also been found to resemble human mucin genes (Celli *et al.* 2005). Porcine gastric and intestinal mucus can be obtained from pig intestines from for example slaughterhouses, which can be a cumbersome process and pose some difficulties. Native mucus is naturally heterogeneous and its composition can vary between individuals and between secretion sites, which can be challenging when comparing results from different studies or even from the same study. For example, Sanders *et al.* reported mucin concentrations that varied from 10 to 47 mg/mL between six samples of natural mucus (Sanders *et al.* 2000). To diminish the individual differences somewhat, mucus from different batches can be mixed. Native gastric and intestinal mucus can also contain various debris like remnants of food and other substances (Groo and Lagarce 2014).

The Caco-2 cell line is often used in studies for drug uptake in the intestine because they are similar to the enterocytes found there. However, there are some difficulties regarding the use of the Caco-2 cell line with mucus. In order to represent the uptake of drugs in human intestines accurately, a mucus layer must be present, but Caco-2 cells are not compatible with native mucus, as it breaks the single-cell layer (Boegh *et al.* 2013, Boegh *et al.* 2014).

Commercial porcine mucin has been used to prepare mucin solutions as a substitute for native mucus, since native mucus can be very diverse and difficult to obtain. Such solutions are more stable, but the results are not necessarily comparable to native mucus, since native mucus contains many other substances, like lipids, salts and other proteins, in addition to mucin (Cone 2009). In addition, the structure of Sigma mucin differs from the mucin found in native mucus. The Sigma mucin is "obtained by digestion of hog stomach with pepsin, followed by precipitation and other steps (Sigma-Aldrich 2011)." The structure of the Sigma mucin has possibly been altered and fragmented by the processes it went through during the isolation, particularly the digestion with pepsin. The extraction process causes disruption of the disulfide bridges between and within the mucin molecules, which results in a weaker gel (Groo and Lagarce 2014). In a study, the diffusion percentage of drugs in native porcine intestinal mucus and purified porcine gastric mucin was found to be significantly different, with the drugs being more hindered by the native mucus. This was attributed to the fact that a mucin-only gel does not accurately reflect the complexity and composition of native mucus (Larhed *et al.* 1997). However, since the two types of mucin that were compared (intestinal mucus and gastric mucin) are from different sites and therefore inherently different, that could be another explanation. Consequently, researchers have directed their focus towards reconstituted mucus, and several types have been made. Some common features are mixing porcine mucin with bovine serum albumin (BSA), buffers, and/or lipids in order to achieve an artificial mucus that is comparable with natural mucus, but without some of its flaws like the high degree of heterogeneity (Groo and Lagarce 2014).

### 1.2.3 Biosimilar mucus

As described above, a mucus model for drug absorption studies that was compatible with Caco-2 cells was lacking. Biosimilar mucus was developed to serve as a biocompatible model for porcine intestinal mucus (PIM), and mimic its rheological properties. Boegh *et al.* prepared and analysed a mixture with inspiration from Larhed *et al.*, who had determined that the main constituents of intestinal mucus was mucin, linoleic acid, cholesterol, phosphatidylcholine (PC) and albumin (BSA) (Larhed *et al.* 1998). Their analysis found that the initial mixture was not successful in reproducing the rheological properties of porcine intestinal mucus, as the mucus mixture displayed liquid-like properties in contrast to the solid-like properties displayed by PIM (Boegh *et al.* 2013). They modified the initial mucus by increasing the mucin content and adding polyacrylic acid (PAA) to obtain shear thinning and solid-like properties comparable to those of porcine intestinal mucus.

PAA is not a part of the natural composition of native mucus, but was needed for the biosimilar mucus to resemble the viscoelastic properties of native mucus. When testing the biocompatibility of the mixture they found that the high content of linoleic acid was toxic to the cells, and thus had to be reduced (Boegh *et al.* 2014).

The rheological properties of the biosimilar mucus were found to be preserved without adding the lipids (linoleic acid, cholesterol and PC), but cryo-SEM imaging showed that the structure of biosimilar mucus was more similar to PIM when the lipids were added (Figure 1.2.3.1). In addition, native mucus contains some lipids, and these are thought to influence the diffusion of drugs through mucus, so including the lipids would give the biosimilar mucus a composition closer to native mucus (Boegh *et al.* 2014).

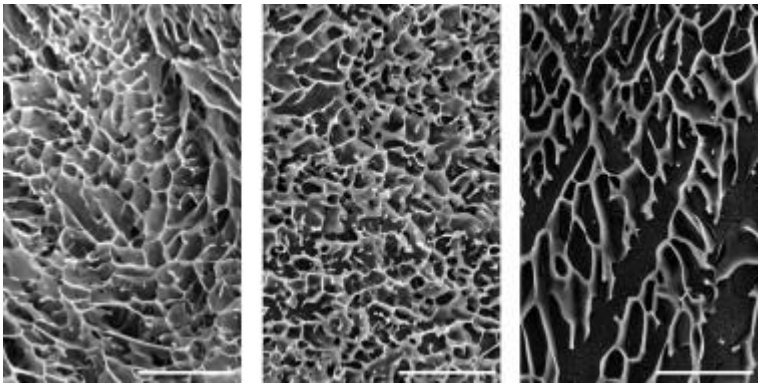

*Figure 1.2.3.1: Cryo-SEM pictures of biosimilar mucus with lipids (left), without lipids (right) and porcine intestinal mucus (middle). Scale bars represent 25 µm (Boegh et al. 2014).*

The final biosimilar mucus composition used by Boegh *et al.* was 5 % (w/v) mucin, 0.9 % (w/v) PAA, 3.1 % (w/v) BSA, 0.65 % (w/v) lipid mixture with 0.11 % (w/v) linoleic acid, 0.36 % (w/v) cholesterol and 0.18 % (w/v) PC in 0.163 % (w/w) polysorbate 80. Analysis of this mucus mixture found that its rheological properties were very much similar to porcine intestinal mucus, and biocompatibility tests assured that the mixture was compatible with living cells. The barrier properties of the biosimilar mucus were tested with both hydrophobic and hydrophilic compounds, and it was found that the mucus hindered the permeability and diffusion of the molecules (Boegh *et al.* 2014). However, no compounds of nanoparticle size were tested.

Since the biosimilar mucus is compatible with the Caco-2 cell line in contrast to native mucus, and represents the complexity of mucus content and structure better than a mucin-only gel, it is a possible candidate for use in drug absorption studies in the small intestine, and possibly in other areas. In addition, the problems with heterogeneity in native mucus, both within and between samples, are circumvented. Every batch of biosimilar mucus will be approximately the same, assuming the same protocol is used, and the equipment and ingredients used are readily available and relatively cheap. However, a more in-depth testing of the barrier properties of biosimilar mucus towards bigger particles like nanoparticle drug delivery systems is needed. In addition, the use of Sigma mucin in the preparation of biosimilar mucus has been proposed as a possible source to some differences found between biosimilar mucus and porcine intestinal mucus (Reehorst 2014). As described earlier, the structure of the Sigma mucin differs from the mucin found in natural mucus because of the extraction process, which causes disruption of the disulfide bridges between and within the mucin molecules (Groo and Lagarce 2014). This would result in a weakening of the mucin network and thus a weaker mucus gel. This theory is supported by the fact that Boegh *et al.* found that a mucus containing Sigma mucin alone did not accurately resemble the viscoelastic properties of PIM, but that addition of PAA was needed (Boegh *et al.* 2014).

## 1.3 Nanoparticles

Nanoparticles are particles whose size are measured in nanometres (nm, $10^{-9}$ to $10^{-7}$ meters). Nanoparticles and nanotechnology have many exciting uses, but this thesis will be focused on the use of nanoparticles as drug delivery systems. Nanoparticles for medical applications are defined as follows:

> *Nanoparticles for pharmaceutical purposes are defined as solid colloidal particles ranging in size from 1 nm to 1000 nm. They consist of macromolecular materials and can be used therapeutically as drug carriers, in which the active principle (drug or biologically active material) is dissolved, entrapped or encapsulated, or to which the active principle is adsorbed or attached.* (Petros and DeSimone 2010).

Nanoparticle drug delivery systems (NDDS) have been on the market for about 20 years, and there are many different types (Grazú *et al.* 2012). In the US, there are at least 15 pharmaceuticals using nanotechnology that have been approved since 1990 (Bamrungsap *et al.* 2012). Nanoparticles can resemble macromolecular compounds like large proteins in size, and can use cellular mechanisms intended for these compounds to move around the body. A variety of nanoparticles can be engineered, depending on the desired properties of the finished NDDS. Some important effects of nanoparticle engineering can be increased bioavailability, stability and solubility, improved pharmacokinetics, increased circulation life, reduced toxicity and decreased adverse effects (Bamrungsap *et al.* 2012, Lee *et al.* 2015).

Drugs can be encapsulated in, dispersed in, adsorbed or conjugated to nanoparticles. Liposomes or polymers filled with, or bonded to the desired drug are some examples. See Figure 1.3.1 for an overview of different types of nanoparticles for drug delivery. NDDS can be modified to affect solubility, stability, permeability, or other properties, leading to improved bioavailability and an enhanced, controlled or more rapid therapeutic effect. The modification can for example be done with coatings or attachment of ligands. Attachment of ligands like antibodies or use of magnets can be methods of targeting drug delivery to specific sites (Bamrungsap *et al.* 2012).

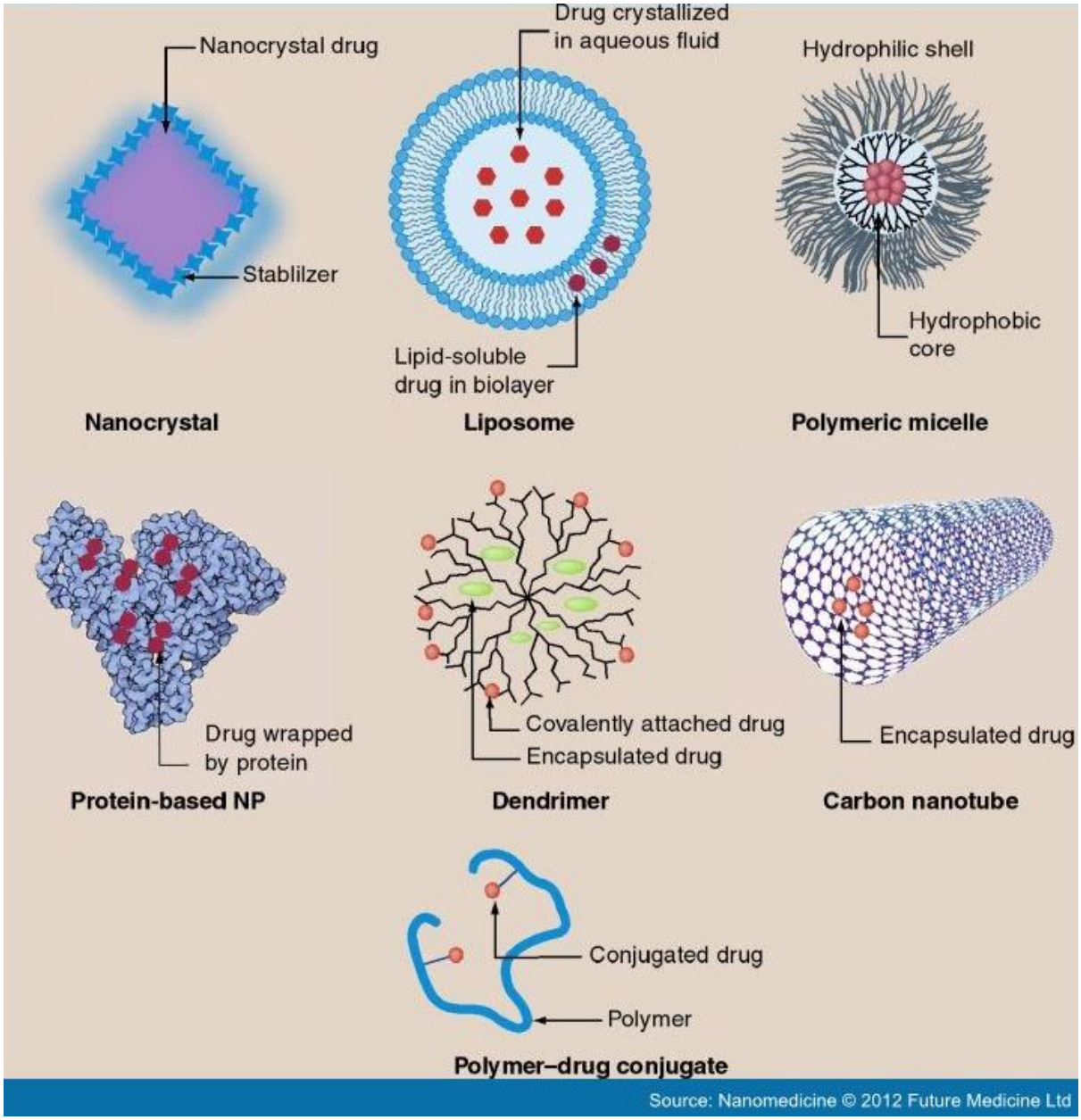


*Figure 1.3.1: An overview of some of the different types of nanoparticles for drug delivery. Included in the figure are nanocrystals, liposomes, polymeric micelles, protein-based nanoparticles, dendrimers, carbon nanotubes and polymer–drug conjugates (Bamrungsap et al. 2012).*

NDDS are especially interesting for the formulation and delivery of biologicals/biopharmaceuticals, which are macromolecular drugs like proteins, nucleic acids or other polymers. The pharmaceutical industry has seen a shift from traditional small molecule drugs towards the development of biologicals for a range of diseases in the last decades, for example in cancer treatment. However, biologicals often have problems with stability and circulation life in the body, since they are easily broken down and metabolised. This is particularly relevant for oral administration, which is often desired for convenience, but which poses many challenges in the form of a harsh environment and extensive metabolism. As mentioned, NDDS can be used for example to increase the stability or circulation life of biologicals in the body, or target them to a specific organ or cell type. Using nanotechnology in targeting drugs for cancer treatment has been especially focused on (Lee *et al.* 2015). By encapsulating the biopharmaceutical in a NDDS it could be protected from degradation and ideally pass through the GI tract unharmed (Wong 2010, Ensign *et al.* 2012).

The targeting of the drugs to their site of action and the increased bioavailability can open up possibilities for administering lower doses of drugs at a time because of decreased loss of drugs and increased efficiency (Bamrungsap *et al.* 2012). Lower doses of drugs are generally desired because of decreased costs and reduced side effects (Orive *et al.* 2004, Laroui *et al.* 2012). Cost-effectivity is particularly applicable in the case of biologicals because these are generally more expensive to produce than traditional small molecule drugs.

### 1.3.1 Nanoparticle mobility in mucus

As explained, nanoparticle drug delivery systems can be modified to enhance their properties in order to deliver drugs like biopharmaceuticals to the body. However, with oral administration, the nanoparticle would still need to pass through the mucus layer of the small intestine in order to enter the circulation and get the biological to its site of action (assuming the site of action is not the GI tract itself). If the nanoparticle fails to interact with the mucus layer at all, it would travel through the intestine and be removed from the body in the faeces. This is often the fate of orally administered nanoparticles (Lai *et al.* 2009a). Alternatively, the nanoparticle could interact with the mucus layer and become trapped, followed by removal from the body as the mucus layer is constantly shed and replenished. Only penetration and diffusion through the mucus layer will enable the nanoparticle to enter the body (Florence 1997, Ponchel and Irache 1998). Engineering nanoparticles specifically to be able to diffuse quickly through the mucus layer is therefore a highly relevant subject (Ensign *et al.* 2012). Important properties that will influence the mobility of nanoparticles in mucus are the size and surface modification (electric charges, hydrophilic or hydrophobic surfaces), and eventual ligands (Norris and Sinko 1997).

Because of the composition and structure of mucus and especially the mucins, the mucus layer is well adapted to trap particles with varying surfaces (Cu and Saltzman 2009). Nanoparticles with positive charges are likely to be attracted to the negatively charged groups in the oligosaccharide side chains of the mucins, for example the carboxylate and sulphate groups. Negatively charged particles would interact with positively charged parts of the mucins, for example amino acid residues carrying a positive charge. Nanoparticles with surfaces containing hydrogen atoms bound to an electronegative atom (O, N) could interact with nearby molecules through hydrogen bonding. Nanoparticles with hydrophobic surfaces would be attracted to the naked and hydrophobic parts of the mucin molecules.

Nanoparticles of larger size will have the ability to carry more drug molecules, and often show a more suitable drug-release kinetic profile where the drug is released over a longer time scale compared to smaller drug-carrying nanoparticles. However, large nanoparticles risk becoming trapped in the mucus layer because of the pore size formed by the interacting mucin molecules. Thus, even a nanoparticle engineered to have a surface chemistry that allows it to avoid mucoadhesion in order to achieve rapid diffusion through mucus, could be hindered and expelled from the body because of an overly large size (Lai *et al.* 2009a).

## 1.4 PEGylation

PEGylation is the technique of covalently attaching polyethylene glycol (PEG), a hydrophilic polymer, to the surface of another molecule or particle with the intention of changing its physical and/or chemical properties. PEGylation is especially attractive to pharmaceutical companies, and it is used as a method in drug delivery, especially with large hydrophobic molecules. The outcome of PEGylation can vary with the original molecule, the method used, and the density and length of the PEG molecules. The results can be, among others, increased water solubility, increased stability, increased circulation time and prolonged lifetime in the body (McDonnell *et al.* 2013, Lee *et al.* 2015). PEGylation can also change or mask the charge or hydrophobic sites of the original substance,

since PEG is a neutral and hydrophilic polymer. However, PEGylation of a drug-carrying nanoparticle can mask eventual targeting peptides on the nanoparticle's surface, meant to interact for example with ligands on the cell membrane of the target cell, and this could cause a reduced uptake to the cell and therefore a reduced efficiency of the therapy. Likewise, PEGylation can also cause reduced biological activity of the drug, since it cannot easily interact with other molecules. An example could be a PEGylated drug whose mechanism of action involves an enzymatic reaction, but the coating with PEG hinders the drug from interacting with the enzyme. Heterogeneity is also a problem because a drug treated with PEGylation can have a number of different binding sites for PEG, and the result is a mixture of heterogeneous PEGylated substances that will behave dissimilarly (McDonnell *et al.* 2013). Other drawbacks that have been proposed and discussed are the immunogenicity of PEG, hypersensitivity to PEG in patients and possible formation of anti-PEG antibodies. Zhang *et al.* highlights the need for further research and more data to expand the knowledge of possible negative effects of the increasing use of PEGylation in the pharmaceutical industry (Zhang *et al.* 2014).

PEGylation of nanoparticles has been proposed as a method of avoiding mucus entrapment, and may also cause the nanoparticles to be more stable in mucus. Lai *et al.* found that covering nanoparticles of varying size with a PEG resulted in an increase of mobility in undiluted mucus (Lai *et al.* 2009a). They also studied the effects of variations in the coating density of nanoparticles and different molecular weight of the PEG molecules. They found that a high-density coverage of low molecular weight PEG (2-5 kDa) was optimal for the transport of the PEGylated particles through mucus. A lower density coverage with PEG led to a dramatic decrease in mobility compared with particles with a high-density coverage, and the same result was found for well-coated particles with 10 kDa PEG molecules (Lai *et al.* 2009a). Another study found that particles with a neutral charge, like PEG, had higher mobility than charged particles in CF sputum (Dawson *et al.* 2003). Some microorganisms have evolved to present an overall neutral but highly hydrophilic surface by coating themselves with proteins, and this reduces their interaction with the components of mucus and increases their permeability and mobility in mucus (Cone 1999).

Stability is particularly an issue for drug delivery in the GI tract, with its the harsh environment and varying pH. Liposomes have been demonstrated to be unstable in the GI tract (Chia-Ming and Weiner 1987, Rowland and Woodley 1980). Studies with PEGylation of lipoplexes (liposomes carrying DNA) have found that the PEGylated lipoplexes did not have interactions with mucus components, and that they had increased gene transfection activity compared to the untreated lipoplexes (Sanders *et al.* 2002, Sanders *et al.* 2003). Yoncheva *et al.* showed that PEGylation of polylactide nanoparticles increased their stability in gastric fluid (Yoncheva *et al.* 2005).

## 1.5 MUCOVA

Alginate is a polysaccharide produced by brown algae (Phaeophyceae). Alginate is a linear polymer comprised of the monomers β-D-mannuronic acid (M) and α-L-guluronic acid (G), whose structure can be seen in Figure 1.5.1. The length and composition of alginate can vary. Regions of the polymer only comprised of β-D-mannuronic acid are often called M-blocks, while regions of α-L-guluronic acid are known as G-blocks. Similarly, regions of alternating mannuronic and guluronic acid are called MG-blocks. Alginate can form gels in the presence of divalent cations like $Ca^{2+}$, and is commonly used in food and other products (Smidsrød and Moe 2008).

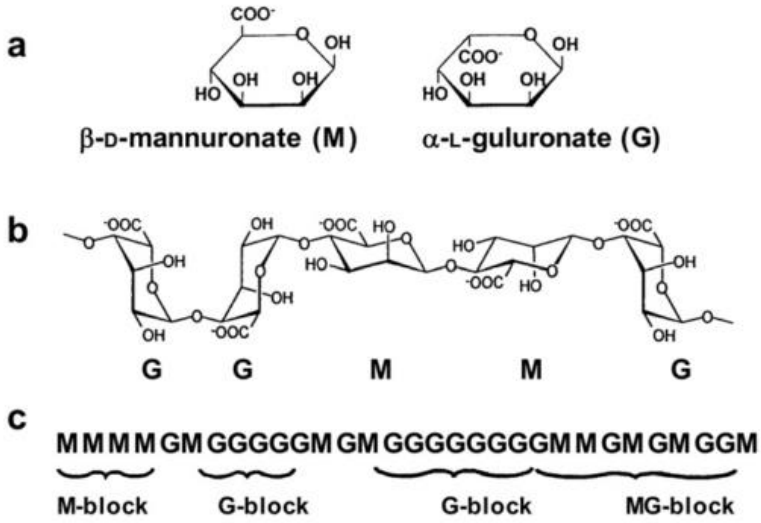


*Figure 1.5.1: The structure of alginate. A: alginate monomers, β-D-mannuronate and α-L-guluronate, often abbreviated to M and G, respectively. B: chain conformation. C: block distribution, with M-blocks, G-blocks and MG-blocks (Draget and Taylor 2011).*

MUCOVA is a G-block technology for mucosal drug delivery for large molecules and delivery vehicles, developed by Nordgård and Draget. MUCOVA consists of G-blocks, which are short oligomers of L-guluronic acid. The G-blocks do not alter the nanoparticle. Instead, they transiently modify the mucus barrier by decreasing the interactions between the mucins within the mucus network, causing an expansion of the pore size.

There are *in vitro* and *ex vivo* data demonstrating that G-blocks improve nanoparticle mobility in mucus and cellular uptake of nanoparticles (Nordgård *et al.* 2014). Adding low molecular weight G-blocks to porcine gastric mucin gels, PSIM and human cystic fibrosis sputum has been shown to weaken the structure of the mucus (Draget 2011, Draget and Taylor 2011, Nordgård and Draget 2011, Nordgård *et al.* 2014, Taylor *et al*. 2007). The G-blocks are thought to interact with the mucus through electrostatic interactions, as they have a negative charge and would be attracted to the positively charged regions of the mucin molecules (Nordgård and Draget 2011). This could mask these regions and hinder them from interactions with other mucus components, for example other mucins, thus reducing the crosslinks in the mucus network.

MUCOVA is one of the contributions to the innovative medicines initiative COMPACT project (Collaboration on the Optimization of Macromolecular Pharmaceutical Access to Cellular Targets) which has the aim of enabling successful delivery of biopharmaceuticals and includes work packages focused on mucosal delivery in the lung and gastrointestinal tract.

## 1.6 Multiple particle tracking

Multiple particle tracking (MPT) is a technique using video microscopy to track the motions of multiple individual nanoparticles over time. In this case, the videos will be obtained using confocal laser scanning microscopy (CLSM), which is a method of acquiring images or videos of high quality. The unique feature of CLSM compared to conventional laser microscopy is its depth selectivity, in other words, its ability to focus the image on a certain depth in the studied sample (Pawley 2006). CLSM is commonly used in biological application, in which case the sample or particular parts of the sample are often fluorescent (Fellers and Davidson 2007). In this case, the sample is fluorescent nanoparticles mixed with mucus. Fluorescent nanoparticles are excited by a light beam corresponding to the specific wavelength absorbed by the particles. The electrons in the

nanoparticles absorb the light by changing conformation and entering a temporary excited state. When the electrons fall back to their lower energy state, the excess energy is released as light with specific wavelengths. This emission of light is detected and used to determine the position of the particles.

In a confocal laser scanning microscope used with a fluorescent sample, an excitation laser beam with a selected wavelength is ran through a filter and focused with a lens into a small area of the sample. This excites the fluorescent parts of the sample, which produces fluorescent light that passes back through the lens together with some scattered light from the laser. A filter lets the light with fluorescent wavelength pass through, while blocking the scattered light of the original wavelength. A pinhole aperture in front of the detector only allows the in-focus light rays from the selected depth to pass through, and not the out-of-focus light from the other depths. This light is then detected by a photodetection device. The detector is connected to a computer, which can be used to visualise, process, analyse, and capture images or videos of the sample (Fellers and Davidson 2007). A schematic drawing of a confocal laser-scanning microscope can be found in Figure 1.6.1.

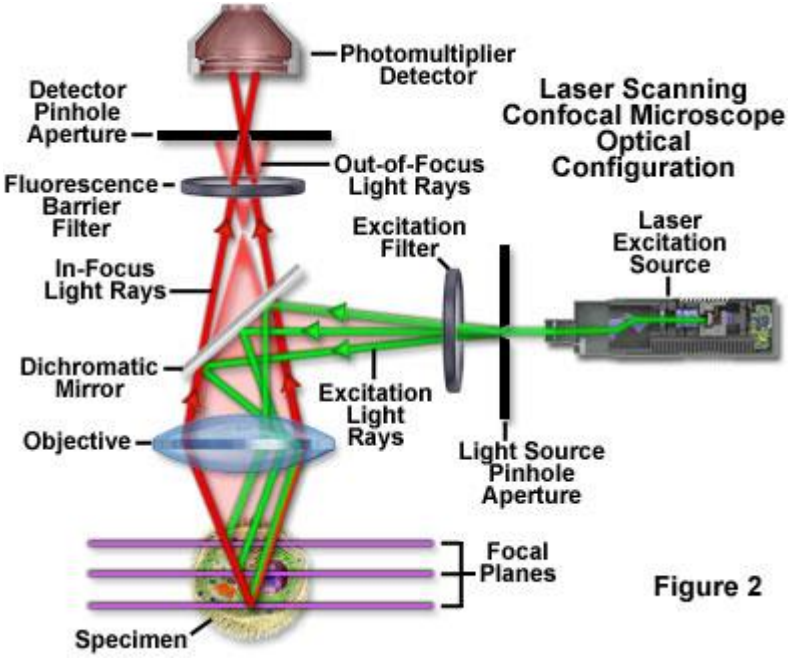


*Figure 1.6.1: Schematic drawing of a confocal laser-scanning microscope (Fellers and Davidson 2007).*

In traditional fluorescence microscopy, the entire sample is exposed to excitation light, and the fluorescent light emitted from the sample can be viewed. This technique gives an image covering a large depth range, and includes out of focus objects and blurring. Filtering the emitted light through a pinhole like in CLSM causes the light that passes through the objective lens to be focused on a certain depth or focal plane in the sample, as shown in Figure 1.6.1. This gives a high-resolution and focused image of the depth plane of interest (Fellers and Davidson 2007). The emitted light from the fluorescent particles is used to register their position (x-, y- and z- coordinates) in the sample. Since this is done for each frame captured, a plot of the particles' movements in the XY plane over time is recorded. It is also possible to scan an entire sample if it is desired to obtain a full 2D or 3D image (Furrer and Gurny 2010). The major disadvantage of CLSM is the expensive equipment needed and the high maintenance costs (Fellers and Davidson 2007).

Multiple particle tracking is done by obtaining the spatiotemporal position (coordinates and time) of fluorescent nanoparticles in a medium as described above, and using mathematical equations to

convert the position data into parameters describing the mobility of the nanoparticles in the medium. When comparing the results of unmodified and modified nanoparticles, one can investigate whether there are significant changes to the mobility of the modified particles (Draget and Nordgård 2014).

MPT makes use of the concept of time scale. In this case, the videos that were captured using CLSM were 6.8 seconds long and contained 100 frames. The time between each frame would then be 68 milliseconds (ms). The first few values of time scale would be 68 ms, 136 ms, 204 ms, 272 ms and so on. The change in nanoparticle position, or displacement values, are recorded for each time scale. The time scale can be described as the period in which a particle is allowed to move before the displacement from an initial point is determined. Thus, a movie of 100 frames would result in 99 displacement values. For each value of time scale, the mean-square displacement (MSD) value can be calculated using the x and y positional data as shown in Eq. (1). MSD (τ) gives information about the distance each particle has travelled from their initial position over time (Suh *et al.* 2005, Selvaggi *et al.* 2010).

$$MSD(\tau) = \langle \Delta x^2 + \Delta y^2 \rangle \quad (1)$$

$\Delta x^2$ and $\Delta y^2$ is the difference between two consecutive sets of x and y positional data, and τ is the time scale. While the initial MSD values at shorter time scales are calculated by taking the means of a generally large number of displacement values, the MSD values at larger time scales are calculated by taking the mean of fewer and fewer displacement values. The last MSD value at the longest time scale consists of just one displacement value. Thus, the MSD values at larger time scales are less statistically accurate (Saxton and Jacobson 1997, Suh *et al.* 2005).

## 2. Aim

The aim of the project is to investigate whether G-blocks can improve mucomobility of PEGylated nanoparticles. It has been shown that G-blocks improve mucomobility of nanoparticles, and that PEGylation is effective as a method of avoiding mucus entrapment. It would be very interesting to look into what effect the combination of these two methods could have on the mobility of nanoparticles in mucus.

# 3. Materials and methods

Multiple particle tracking (MPT) was used to track the motion of fluorescent nanoparticles of different sizes (100 and 200 nm) and with varying surface modification (aminated, carboxylated or PEGylated) in *ex vivo* porcine small intestinal mucus (PSIM) and biosimilar mucus with and without G-blocks.

## 3.1 Materials

100 and 200 nm yellow-green fluorescent carboxylated and aminated nanoparticles (FluoSpheres, 2 % solids) were bought from Invitrogen (Oregon, USA). 1-ethyl-3-(3-dimethylaminopropyl)carbodiimide hydrochloride (EDC) was obtained from Fluka. N-hydroxysulfosuccinimide (Sulfo-NHS), L-α-phosphatidylcholine (PC), linoleic acid, cholesterol, ethylenediaminetetraacetic acid (HEPES), polysorbate tween 80, Sigma mucin type II and bovine albumin were obtained from Sigma-Aldrich Co. (St. Louis, USA). Polyacrylic acid (PAA) was bought from Recklitt & Colman Products (Kingston upon Hull, UK). 2 kDa methoxy-polyethylene glycol-amine (mPEGa) was bought from Creative PEGWorks (Chapel Hill, North Carolina, USA). $CaCl_2$, $MgSO_4$ and NaCl was bought from Merck (Dermstadt, Germany). G-blocks $DP_n$ 12 was produced by acid hydrolysis of an alginate sample as described by Reehorst (Reehorst 2014). The porcine small intestinal mucus (PSIM) was scraped from the small intestines of recently slaughtered pigs (from Gilde's slaughterhouse in Steinkjer), frozen and stored in beakers at -20 °C. Lab-Tek ® Chambered #1.0 Borosilicate Coverglass system, commonly known as 8-well plates, were bought from Thermo Fisher Scientific Inc. (NY, USA).

## 3.2 PEGylation of FluoSpheres

Yellow-green fluorescent carboxylated nanoparticles (FluoSpheres, 200 nm) were PEGylated with a high density of low molecular weight PEG (2kDa) according to protocol (Suh *et al.* 2007), found in Appendix A. A mixture of 2 kDa methoxy-polyethylene glycol-amine (mPEGa, 10 mg), 1-ethyl-3-(3-dimethylaminopropyl)carbodiimide hydrochloride (EDC, 4 mg), and N-hydroxysulfosuccinimide (Sulfo-NHS, 1.13 mg) were dissolved in HBS buffer (0.5 mL, pH 8, 10 mM HEPES, 150 mM NaCl, 3.4 mM EDTA, 0.005 m% Tween 20). FluoSpheres (0.5 mL) were added to the solution and the mixture was left to stir at 200 rpm overnight. The PEGylated nanoparticles were then extracted by centrifugation, and diluted with HBS buffer to a final concentration of 2 %. The bead sizes and zeta potential of a 1:100 diluted PEGylated FluoSphere solution in HEPES buffer (pH 7.3) was measured to assess the effectiveness of the PEGylation reaction using a Zetasizer Nano-ZS (Malvern).

## 3.3 Production of biosimilar mucus

Biosimilar mucus was produced according to protocol (Boegh *et al.* 2013), found in Appendix B.

100 mL 10 mM isotonic HEPES buffer was produced containing 1.3 mM $CaCl_2$, 1 mM $MgSO_4$ and 137 mM NaCl. 100 mL 10 mM non-isotonic HEPES buffer was produced containing 1.3 mM $CaCl_2$ and 1 mM $MgSO_4$.

Lipid solution: 0.0121 g linoleic acid, 0.0396 g cholesterol and 0.033 g phosphatidylcholine (PC) was weighed out and mixed in an Eppendorf tube. 0.03586 g polysorbate tween 80 was weighed out and added to the tube, along with two small magnets. 750 µL of isotonic HEPES buffer (10 mM) was added. The tube was left on vigorous magnetic stirring until the solution was homogenous.

Polymer solution: 0.09 g polyacrylic acid (PAA) was added to 9.168 mL of non-isotonic HEPES buffer (10 mM) and stirred until dissolved. 0.5 g Sigma mucin type II was added and stirred until dissolved. 150 µL 5 mM NaOH was added and the mixture was stirred until visually homogenous.

0.682 mL of the homogenous lipid solution was added, and the mixture was stirred. 0.31 g bovine albumin was added and the mixture was stirred until homogenous. The pH was adjusted from 4.1 to 7.4 with 1 M NaOH and a pH-meter. The biosimilar mucus was made in two batches, and while the first, smaller batch was stored cold (ca 3.5 °C), the second, larger batch was frozen (-20 °C) for later use.

## 3.4 Sample preparation

Approximately 200 mg of the desired mucus (PSIM/biosimilar mucus) was weighed out in chambers on an 8-well plate. The PSIM or biosimilar mucus used in preparation of one set of samples came from the same batch. This was to minimize uncertainty caused by individual differences in mucus composition.

FluoSpheres were added to mucus to a final concentration of nanoparticles of 0.0025 %. This was done by diluting the desired particles (2 % solids) 1:40 in G-block solutions or physiological saline (control). The control is added saline to balance out the ionic strength of the G-blocks. G-block solutions were prepared with concentration 21 mg/mL, 2.1 mg/mL and 0.21 mg/mL by dissolving G-blocks of $DP_n$ 12 in MQ water. This would give a final concentration of G-block in the prepared mucus sample of respectively 1.0 mg/mL, 0.1 mg/mL and 0.01 mg/mL. 10 µL of the diluted particles were added to the mucus, and stirred with a pipette tip. The 8-well plate was covered with parafilm and lid and stored cool (3 °C) over night, and videos were acquired on Leica SP5 the following day.

## 3.5 Multiple particle tracking

Movement of the fluorescent particles was tracked by MPT. The instrument used was a confocal laser-scanning microscope (CLSM) Leica SP5 from Leica microsystems (Mannheim, Germany). The settings used were 63x1.2 wet objective, Argon laser (20 %), 488 nm laser, detection 520-550 nm. Acquisition mode xyt, with 68 ms between frames and 100 frames total per video. The Leica instrument takes a series of 100 quick images (frames) in 6.8 seconds, forming a short video. The videos were loaded up in the program ImageJ with the plugin SpeckleTracker. This program detects and tracks the trajectory of the individual particles over time. The x- and y-coordinate positions of the individual FluoSpheres were determined for each frame. The coordinate data was converted into mean square displacement (MSD) values using Matlab. The Matlab script used was developed by Astrid Bjørkøy at the department of physics (NTNU) and is given in Appendix D. The MSD (τ) values were calculated as shown in Eq. (1) below.

$$MSD(\tau) = \langle \Delta x^2 + \Delta y^2 \rangle \quad (1)$$

$\Delta x^2$ and $\Delta y^2$ is the difference between two consecutive sets of x and y positional data, and τ is the time scale. Graphs of MSD values with respects to time scale (τ) were drawn.

# 4. Results

## 4.1 PEGylation of FluoSpheres

The zeta potential of a 1:100 diluted PEGylated FluoSphere solution in HEPES buffer (pH 7.3) was measured to assess the effectiveness of the PEGylation reaction. The zeta potential was measured to be about -10 mV, which indicates a successful reaction. Other studies have recorded similar zeta potentials of PEGylated particles, for example Yang *et al.* reports a zeta potential of about −9.6 mV (Yang *et al.* 2012). For comparison, the zeta potential of untreated carboxylated particles is about -43 mV (Nordgård *et al.* 2014). More detailed results of zeta potential and bead size of the PEGylated particles can be found in Appendix E.

## 4.2 Examination of aminated and PEGylated nanoparticle mobility in biosimilar mucus and PSIM

Movement of the fluorescent particles were tracked by MPT as previously explained. During practice with the confocal microscope both porcine small intestinal mucus (PSIM) and biosimilar mucus were used to prepare samples, and when the data was analysed a significant difference in particle mobility between the two types of mucus was found. This influenced the first experiments to be focused on doing a comparison between particle mobility in biosimilar mucus and PSIM.

The mobility of fluorescent 100 nm aminated and 200 nm PEGylated particles in both biosimilar and PSIM were tracked, the data was analysed and graphs of mean square displacement (MSD) of the particles with respect to the time scale were produced, and are shown below in Figure 4.2.1. These particles were chosen for their differences in mucomobility, as 100 nm aminated particles are known to be largely immobile and 200 nm PEGylated particles are known to be largely mobile.

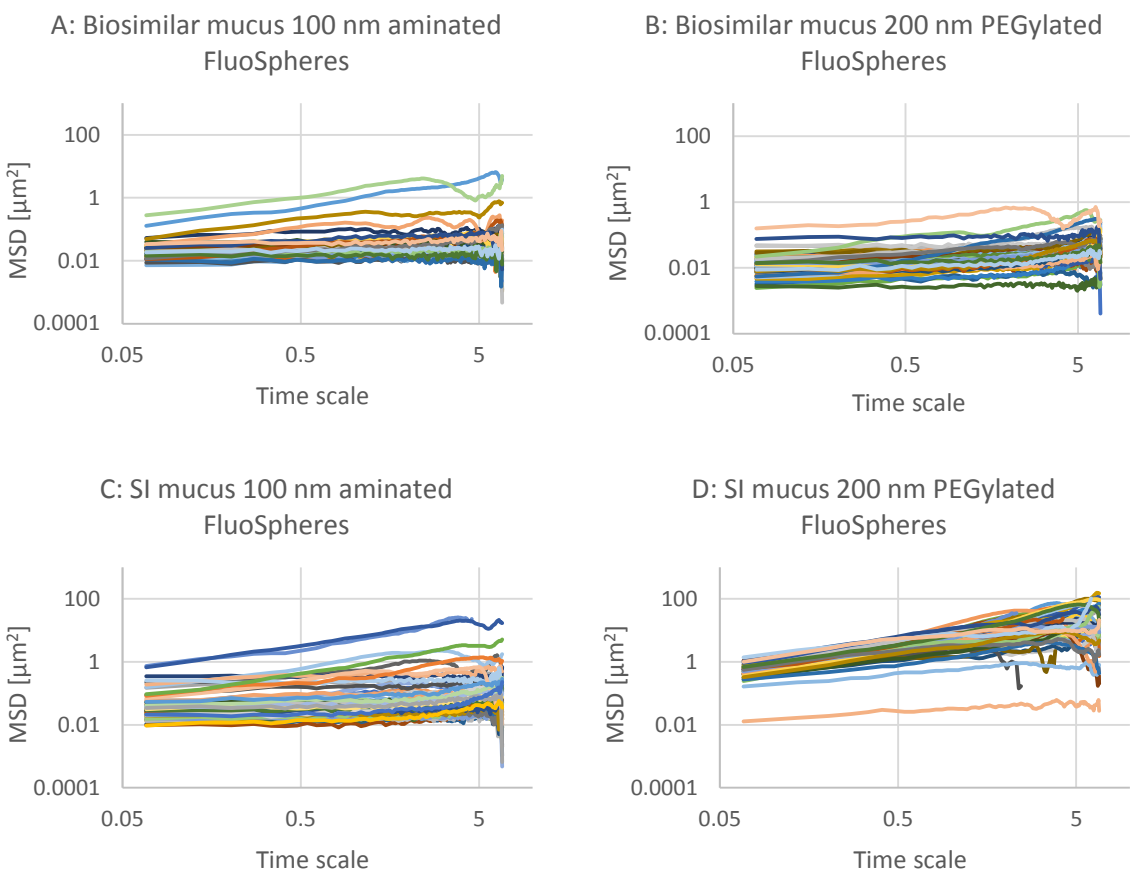


*Figure 4.2.1: Graphs of mean square displacement (MSD) with respect to time scale for four sets (A to D) of FluoSphere nanoparticles in biosimilar mucus and PSIM. The nanoparticles are 100 nm aminated or 200 nm PEGylated particles. There are about 50 trajectories in each graph. Referring to Table 3.4.1, the wells corresponding to the letters are A-3, B-2, C-7, D-6.*

The graphs show that the aminated particles in both types of mucus are relatively immobile, even though there are a few mobile particles. For the PEGylated nanoparticles there is a marked difference in mobility between the biosimilar mucus and the PSIM. The particles are largely mobile in PSIM, with a few immobile particles, but in biosimilar mucus all the particles are immobile. This difference is also illustrated in the mean MSD graph below (Figure 4.2.2). Since the trajectories are mostly similar for each graph, with only a few outliers, a mean is a suitable way of presenting the data.

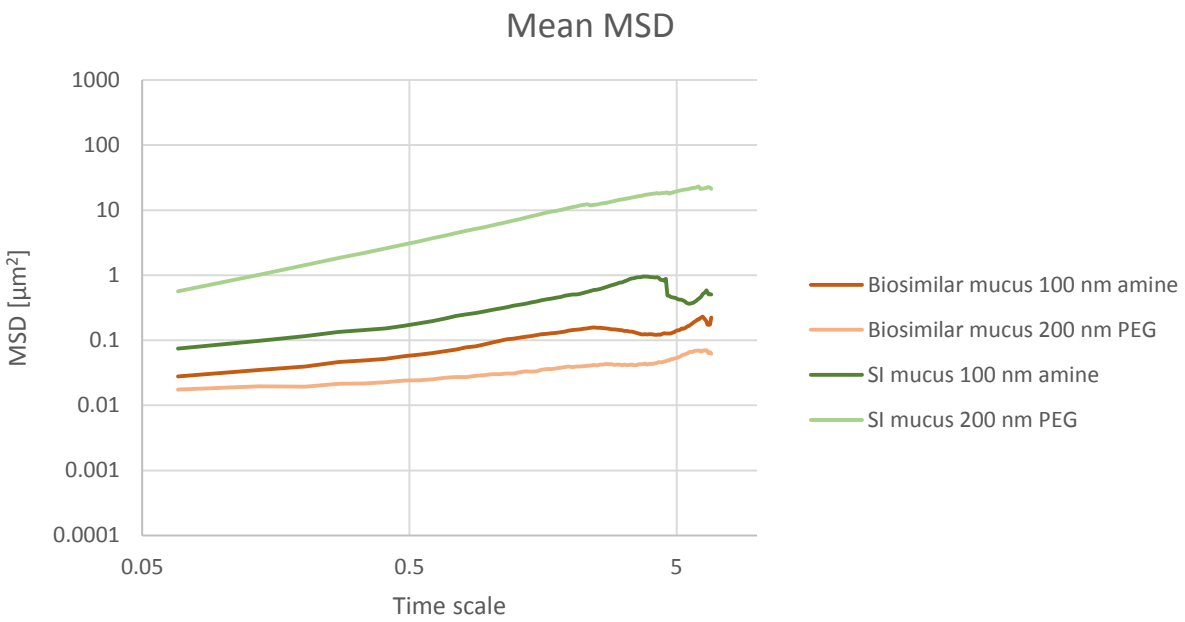


*Figure 4.2.2: Graph of mean MSD values of all the trajectories for the graphs A to D in Figure 4.2.1. The nanoparticles are 100 nm aminated or 200 nm PEGylated particles in PSIM or biosimilar mucus.*

Figure 4.2.2 above highlights the differences observed between particle mobility in biosimilar mucus and PSIM. The 100 nm aminated nanoparticles are immobile in both types of mucus. As can be seen from the figure, the difference between the aminated particles in the two types of mucus are small, but the difference between the PEGylated particles is large. In the biosimilar mucus the PEGylated particles are immobile, while in the PSIM the PEGylated particles are mobile.

## 4.3 Comparison of aminated and PEGylated nanoparticle mobility in biosimilar mucus and PSIM with added G-blocks

The results from the first experiment caused an interest to look deeper into particle mobility in both PSIM and biosimilar mucus, this time with the addition of G-blocks in different concentrations. The particles used were still 100 nm aminated and 200 nm PEGylated particles. In addition, this experiment would allow investigation of G-block effect on PEGylated particles and G-block effect in biosimilar mucus.

A: Biosimilar mucus 100 nm aminated FluoSpheres control

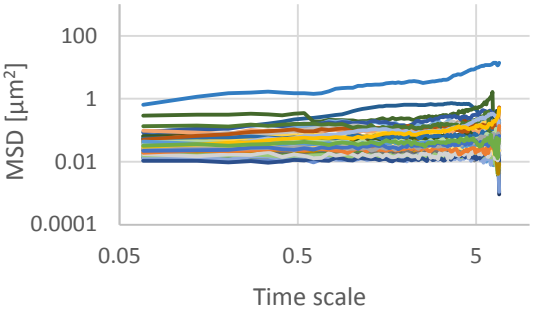


B: Biosimilar mucus 200 nm PEGylated FluoSpheres control

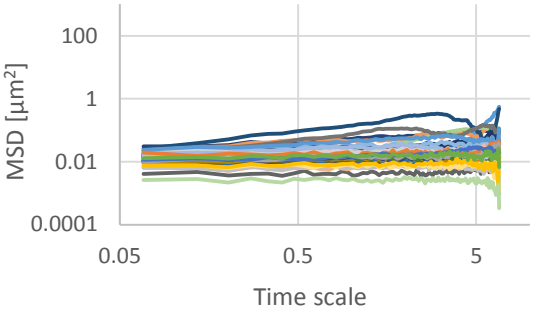


C: Biosimilar mucus 100 nm aminated FluoSpheres 0.01 mg/mL G-block

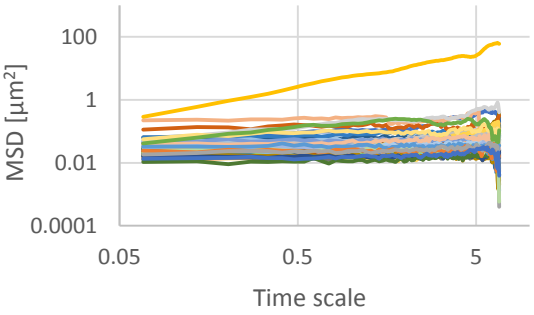


D: Biosimilar mucus 200 nm PEGylated FluoSpheres 0.01 mg/mL Gblock

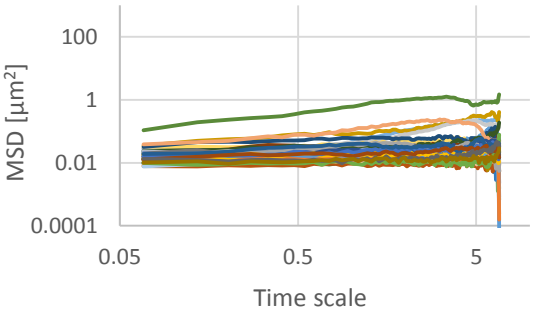


E: Biosimilar mucus 100 nm aminated FluoSpheres 0.1 mg/mL G-block

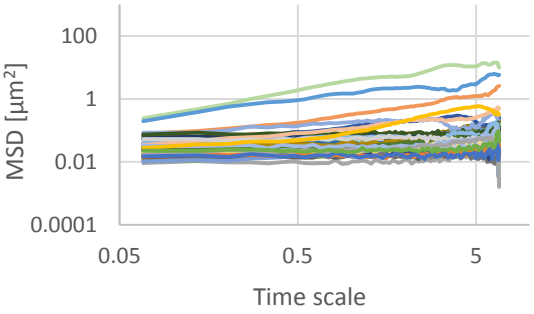


F: Biosimilar mucus 200 nm PEGylated FluoSpheres 0.1 mg/mL Gblock

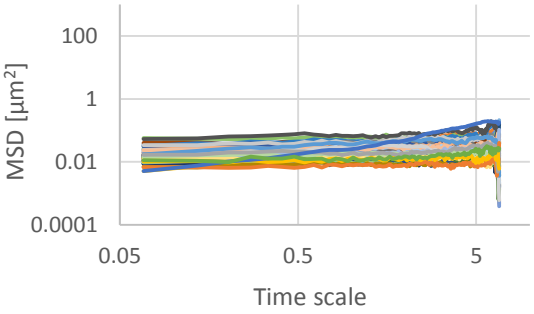


G: Biosimilar mucus 100 nm aminated FluoSpheres 1.0 mg/mL G-block

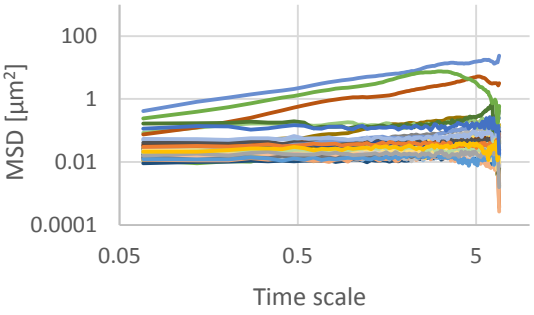


H: Biosimilar mucus 200 nm PEGylated FluoSpheres 1.0 mg/mL Gblock

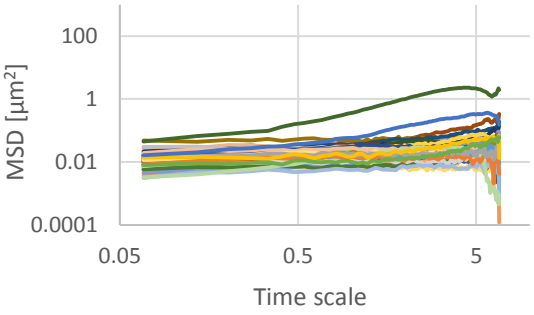

*Figure 4.3.1: Graphs of mean square displacement (MSD) with respect to time scale for eight sets (A to H) of FluoSphere nanoparticles in biosimilar mucus. The nanoparticles are 100 nm aminated or 200 nm PEGylated particles with added G-block in three different concentrations (0.01, 0.1 and 1.0 mg/mL) and a control with physiological saline. There are about 60 trajectories in each graph. Referring to Table 3.4.1, the wells corresponding to the letters are A-8, B-4, C-7, D-3, E-6, F-2, G-5, H-1.*

The results from the experiment with the biosimilar mucus is shown in Figure 4.3.1. The results show that all the particles, regardless of surface modification or addition of G-blocks, are largely immobile. There are a few exceptions, especially with the 100 nm aminated particles, where a few of the sixty measured particles are more mobile than the rest. An overview of the data is shown in Figure 4.3.2, with mean MSD trajectories for each graph from Figure 4.3.1. As mentioned earlier, since almost all the trajectories are in the same area for each graph, a mean is a suitable way of presenting the data.

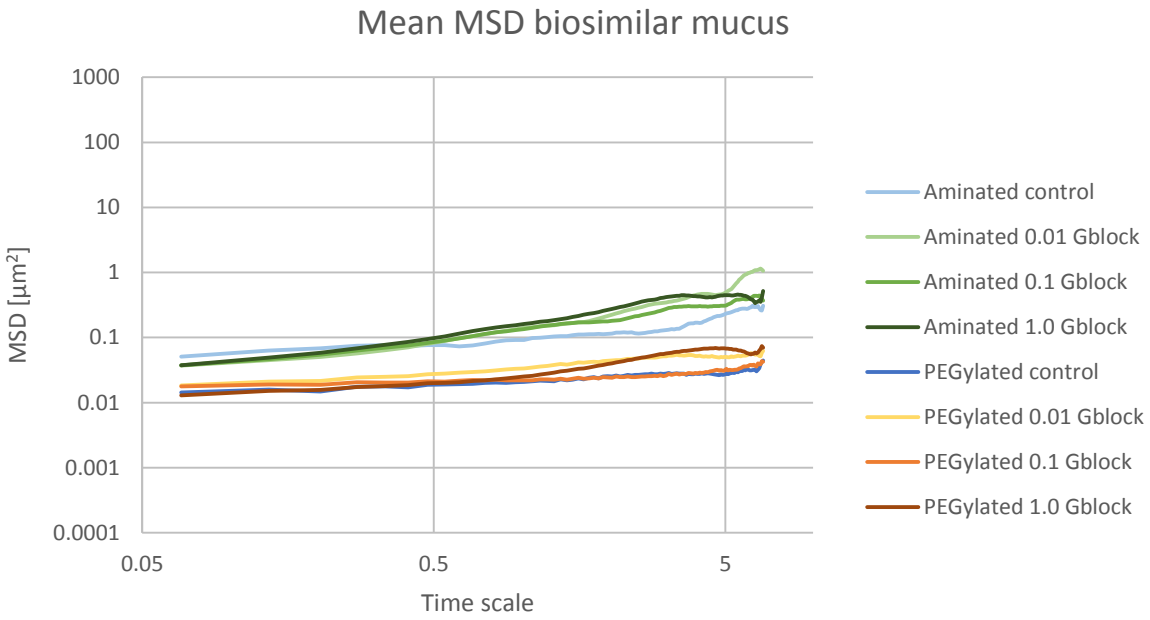


*Figure 4.3.2: Graph of mean MSD values of all the trajectories for the graphs A to H in Figure 4.3.1. The nanoparticles are 100 nm aminated or 200 nm PEGylated particles in biosimilar mucus with added G-block in three different concentrations (0.01, 0.1 and 1.0 mg/mL) and a control with physiological saline.*

The overview of the mean MSD trajectories in Figure 4.3.2 reinforces the impression from Figure 4.3.1. Both the 100 nm aminated and the 200 nm PEGylated particles are overall immobile, with the PEGylated particles being completely stationary. The addition of G-blocks seems to have no marked effect on any of their mobility.

A: SI mucus 100 nm aminated FluoSpheres control

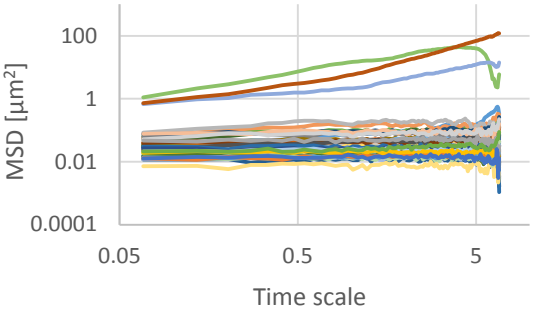


B: SI mucus 200 nm PEGylated FluoSpheres control

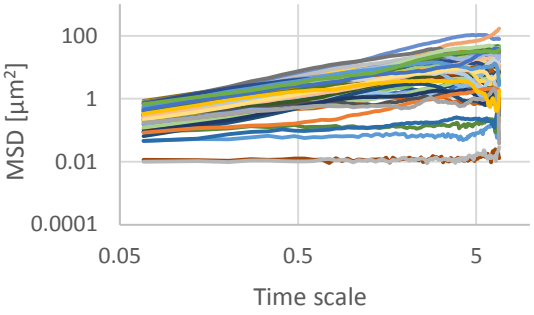


C: SI mucus 100 nm aminated FluoSpheres 0.01 mg/mL Gblock

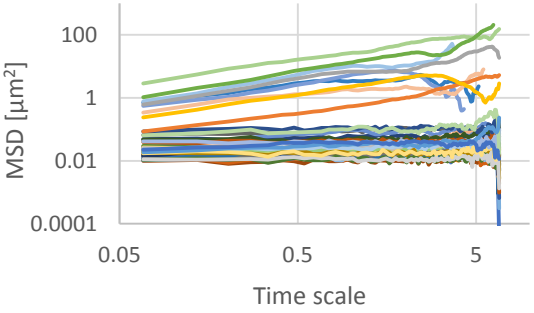


D: SI mucus 200 nm PEGylated FluoSpheres 0.01 mg/mL Gblock

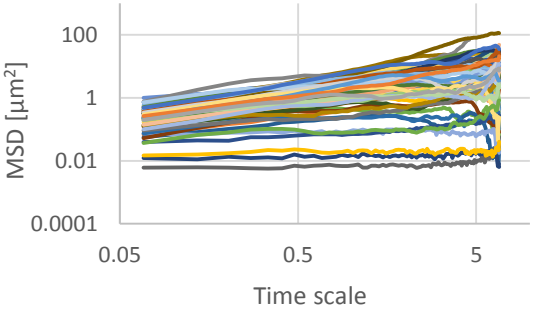


E: SI mucus 100 nm aminated FluoSpheres 0.1 mg/mL Gblock

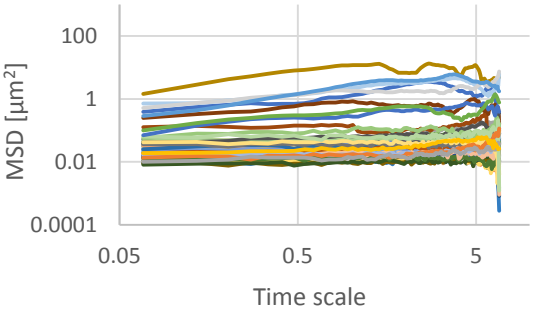


F: SI mucus 200 nm PEGylated FluoSpheres 0.1 mg/mL Gblock

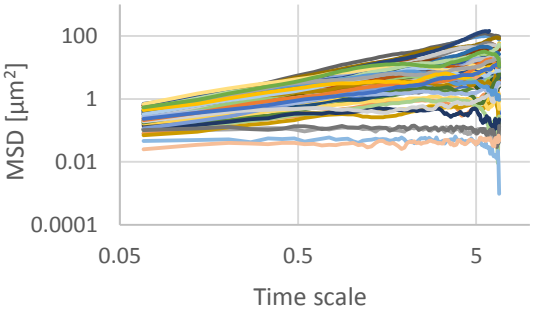


G: SI mucus 100 nm aminated FluoSpheres 1.0 mg/mL Gblock

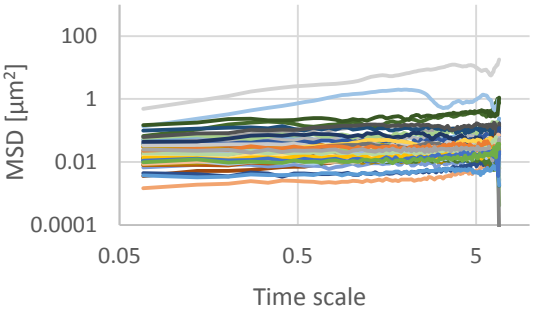


H: SI mucus 200 nm PEGylated FluoSpheres 1.0 mg/mL Gblock

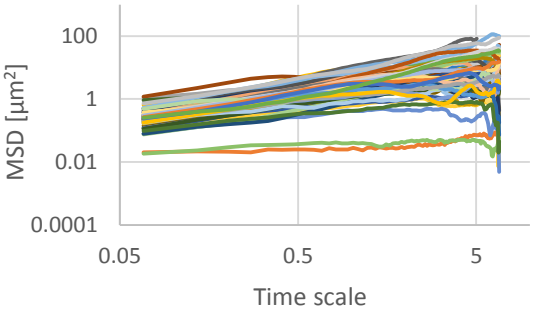

*Figure 4.3.3: Graphs of mean square displacement (MSD) with respect to time scale for eight sets (A to H) of FluoSphere nanoparticles in PSIM. The nanoparticles are 100 nm aminated or 200 nm PEGylated particles with added G-block in three different concentrations (0.01, 0.1 and 1.0 mg/mL) and a control with physiological saline. There are about 60 trajectories in each graph. Referring to Table 3.4.1, and the wells corresponding to the letters are A-8, B-4, C-7, D-3, E-6, F-2, G-5, H-1.*

The results from the experiment with the PSIM are shown in Figure 4.3.3. The results show that the 100 nm aminated particles are largely immobile, with a varying but relatively small fraction of mobile particles. The opposite is true for the 200 nm PEGylated particles, where the particles are mainly mobile with a few immobile exceptions. An overview of the data is shown in Figure 4.3.4, with mean MSD trajectories for each graph from Figure 4.3.3.

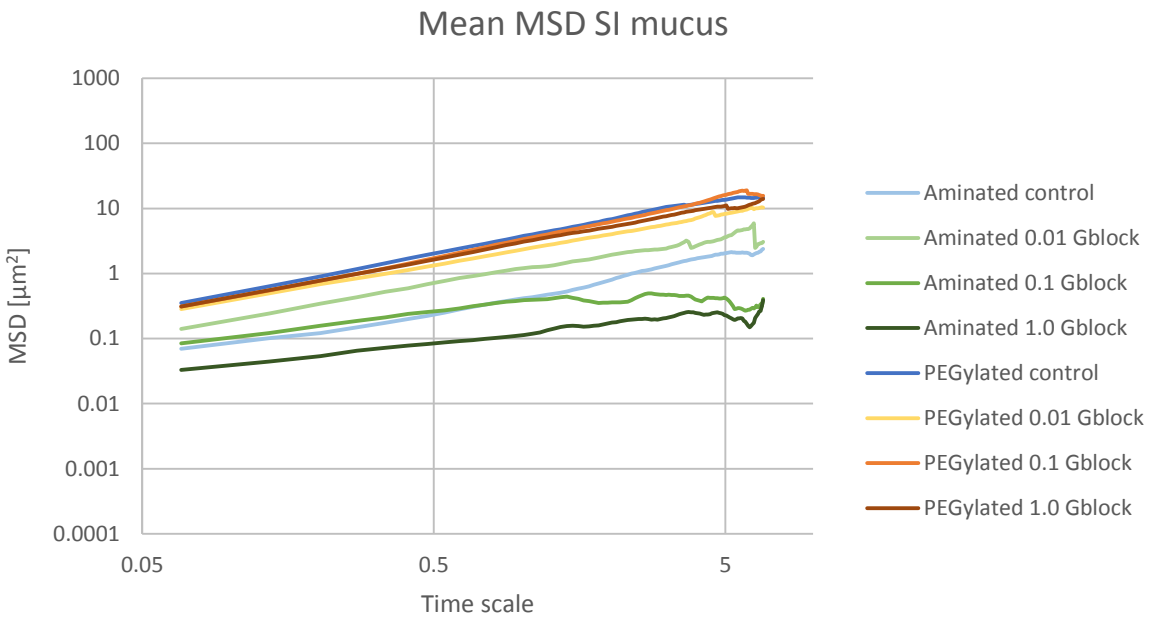


*Figure 4.3.4: Graph of mean MSD values of all the trajectories for the graphs A to H in Figure 4.3.3. The nanoparticles are 100 nm aminated or 200 nm PEGylated particles in PSIM with added G-block in three different concentrations (0.01, 0.1 and 1.0 mg/mL) and a control with physiological saline.*

The overview of the mean MSD trajectories in Figure 4.3.4 shows that the 200 nm PEGylated particles are mobile regardless of the addition or the concentration of G-blocks, and so the addition of G-blocks seem to have no effect on their mobility. The 100 nm aminated particles are a bit more scattered, because of the seemingly random and variable amount of individual mobile particles among the immobile ones, which affects the mean MSD values. However, there seems to be no pattern to the variations, and at first glance there is no marked effect of the G-blocks.

## 4.4 Comparison of same size aminated and PEGylated nanoparticle mobility in PSIM with added G-blocks

After observing the results shown in Figure 4.3.2 and 4.3.4, it was elected to focus more on the effect of G-blocks in PSIM and less on the biosimilar mucus. In this experiment, it was decided to use 200 nm aminated and 200 nm PEGylated nanoparticles, to ensure that the size of the particles would not be a factor when comparing their mobility. See also Figure 4.3.3 for more results of PEGylated nanoparticle mobility in PSIM with added G-blocks, and especially Figure 4.3.4 (which shows graphs of mean MSD value for graphs A to H from Figure 4.3.3).

A: SI mucus 200 nm aminated FluoSpheres control

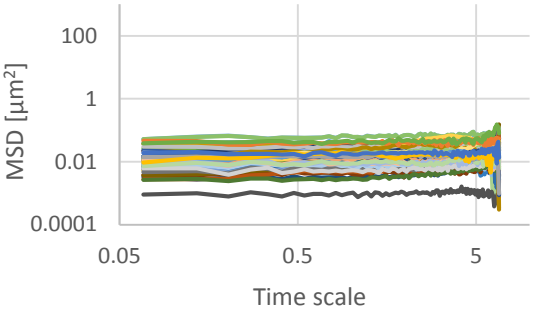


B: SI mucus 200 nm PEGylated FluoSpheres control

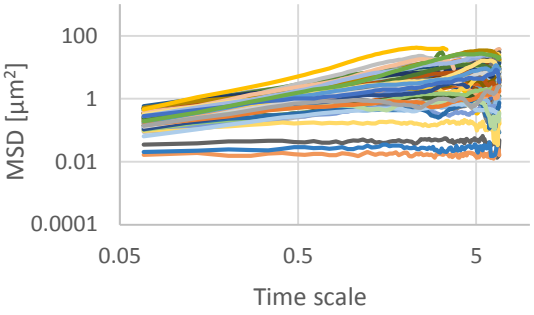


C: SI mucus 200 nm aminated FluoSpheres 0.01 mg/mL Gblock

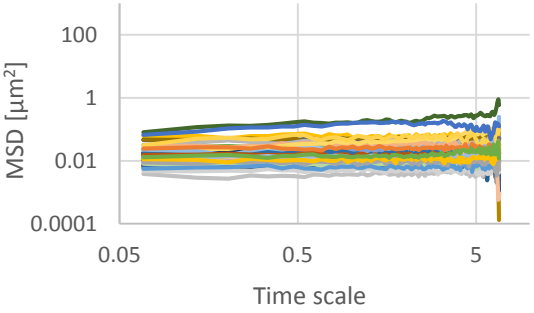


D: SI mucus 200 nm PEGylated FluoSpheres 0.01 mg/mL Gblock

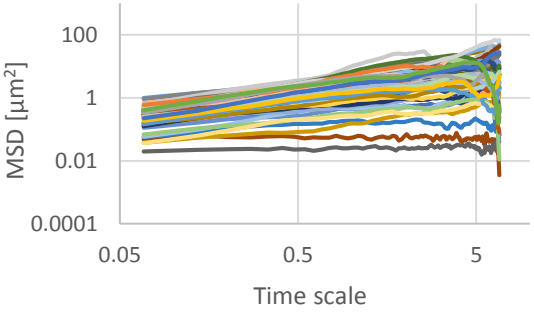


E: SI mucus 200 nm aminated FluoSpheres 0.1 mg/mL Gblock

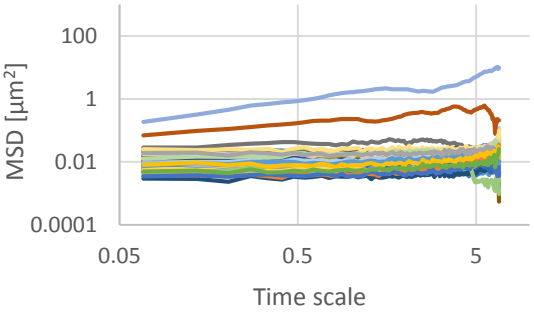


F: SI mucus 200 nm PEGylated FluoSpheres 0.1 mg/mL Gblock

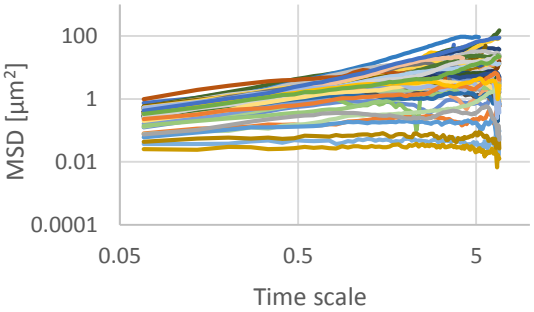


G: SI mucus 200 nm aminated FluoSpheres 1.0 mg/mL Gblock

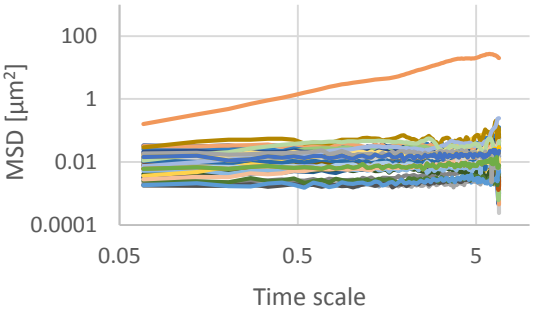


H: SI mucus 200 nm PEGylated FluoSpheres 1.0 mg/mL Gblock

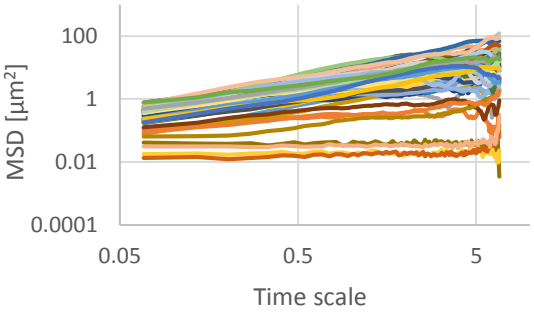

*Figure 4.4.1: Graphs of mean square displacement (MSD) with respect to time scale for eight sets (A to H) of FluoSphere nanoparticles in PSIM. The nanoparticles are 200 nm aminated or 200 nm PEGylated particles with added G-block in three different concentrations (0.01, 0.1 and 1.0 mg/mL) and a control with physiological saline. There are about 60 trajectories in each graph. Referring to Table 3.4.1, the wells corresponding to the letters are A-5, B-1, C-6, D-2, E-7, F-3, G-8, H-4.*

The results from the experiment is shown in Figure 4.4.1. The results show, again, that the 200 nm aminated particles are largely immobile, with one or two mobile particles. The 200 nm aminated particles seem to be less mobile than the 100 nm aminated ones. The 200 nm PEGylated particles are mainly mobile with a few less mobile exceptions. An overview of the data is shown in Figure 4.4.2, with mean MSD trajectories for each graph from Figure 4.4.1.

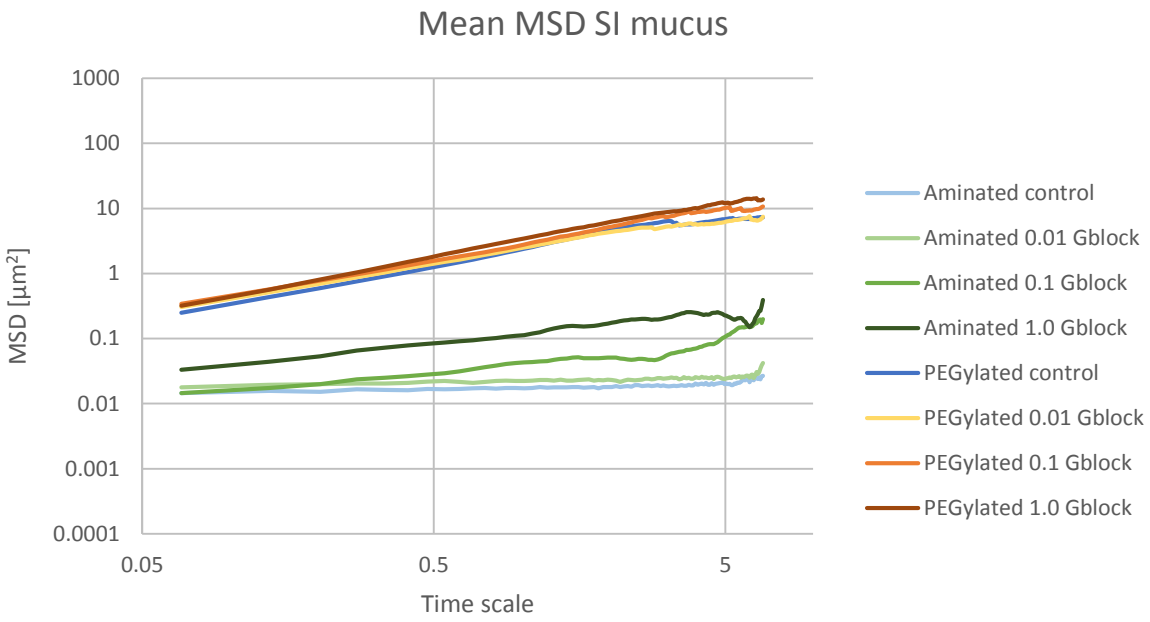


*Figure 4.4.2: Graph of mean MSD values of all the trajectories from graphs A to H in Figure 4.4.1. The nanoparticles are 200 nm aminated or 200 nm PEGylated particles in PSIM with added G-block in three different concentrations (0.01, 0.1 and 1.0 mg/mL) and a control with physiological saline.*

The overview of the mean MSD trajectories in Figure 4.4.2 shows, again, that all the 200 nm PEGylated particles are mobile and that the addition of G-blocks seem to have no significant effect on their mobility. The 200 nm aminated particles are largely immobile, but a small positive effect of the G-blocks can be seen.

## 4.5 Comparison of aminated and carboxylated nanoparticle mobility in PSIM with added G-blocks

A study of the effect of G-blocks on 100 and 200 nm carboxylated particles was a logical next step, in order to observe their mobility and the effect of G-blocks. The 200 nm aminated particles were also included in order to get a second set of data for this type of nanoparticle.

A: SI mucus 100 nm carboxylated FluoSpheres control

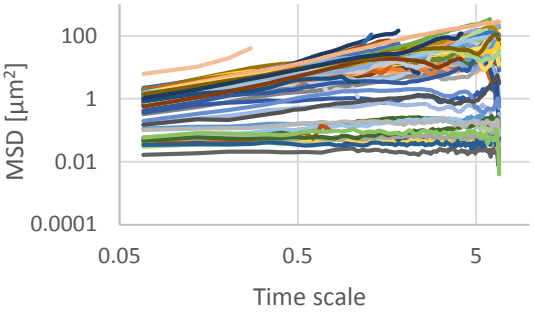


B: SI mucus 200 nm carboxylated FluoSpheres control

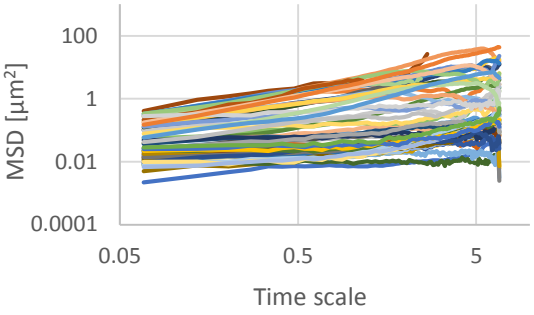


C: SI mucus 100 nm carboxylated FluoSpheres 0.01 mg/mL Gblock

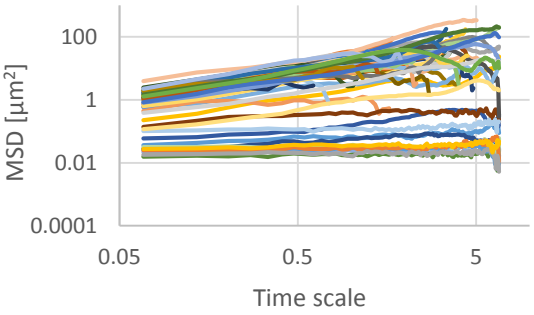


D: SI mucus 200 nm carboxylated FluoSpheres 0.01 mg/mL Gblock

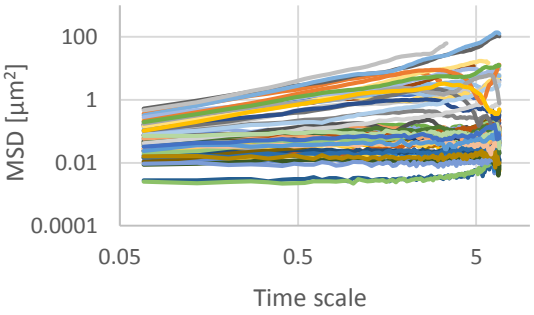


E: SI mucus 100 nm carboxylated FluoSpheres 0.1 mg/mL Gblock

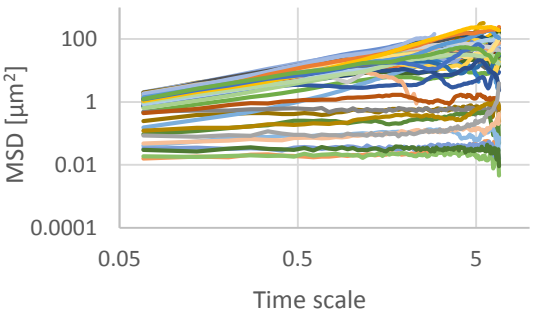


F: SI mucus 200 nm carboxylated FluoSpheres 0.1 mg/mL Gblock

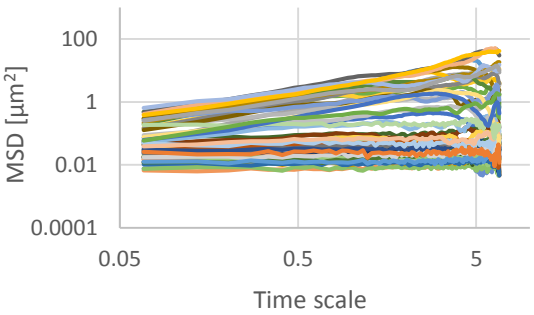


G: SI mucus 100 nm carboxylated FluoSpheres 1.0 mg/mL Gblock

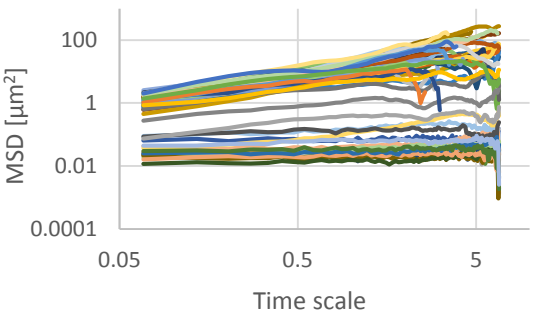


H: SI mucus 200 nm carboxylated FluoSpheres 1.0 mg/mL Gblock

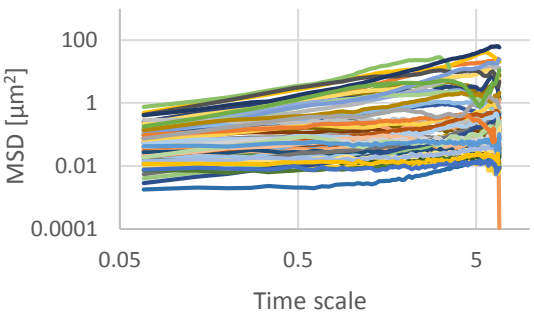

*Figure 4.5.1: Graphs of mean square displacement (MSD) with respect to time scale for eight sets (A to H) of FluoSphere nanoparticles in PSIM. The nanoparticles are 100 or 200 nm carboxylated particles with added G-block in three different concentrations (0.01, 0.1 and 1.0 mg/mL) and a control with physiological saline. There are about 60 trajectories in each graph. Referring to Table 3.4.1, the wells corresponding to the letters are A-2, B-2, C-3, D-3, E-6, F-6, G-7, H-7.*

The results for the 100 nm and 200 nm carboxylated particles are found in 4.5.1. In general, the results for both of the carboxylated particles show greater variation than earlier results for other particles. The particles seem to be divided into two subpopulations, where one is mobile and the other is immobile. For the 100 nm particles the mobile subpopulation is larger than the immobile subpopulation, while for the 200 nm particles the immobile population is the largest.

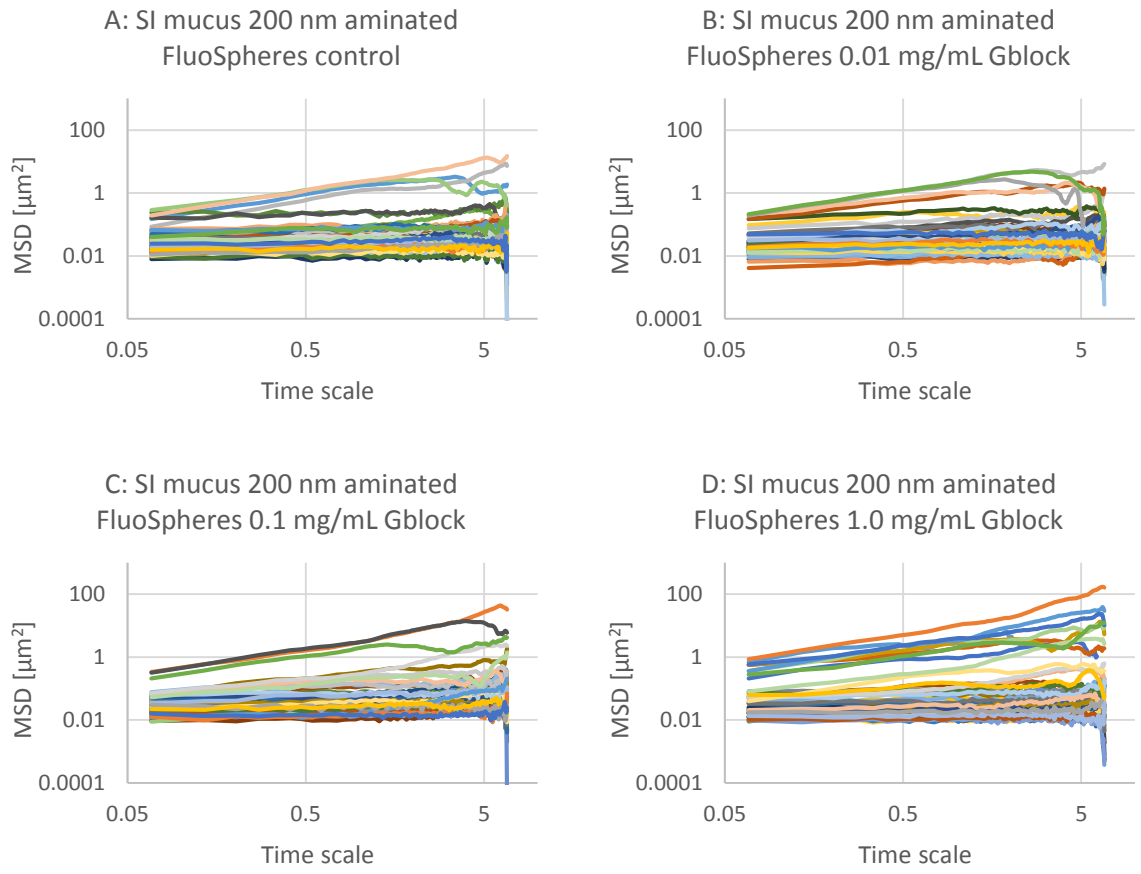


*Figure 4.5.2: Graphs of mean square displacement (MSD) with respect to time scale for four sets (A to D) of FluoSphere nanoparticles in PSIM. The nanoparticles are 200 nm aminated particles with added G-block in three different concentrations (0.01, 0.1 and 1.0 mg/mL) and a control with physiological saline. There are about 60 trajectories in each graph. Referring to Table 3.4.1, the wells corresponding to the letters are A-2, B-3, C-6, D-7.*

The results for the 200 nm aminated particles are shown in Figure 4.5.2. The 200 nm aminated particles are mostly stationary with a small mobile subpopulation.

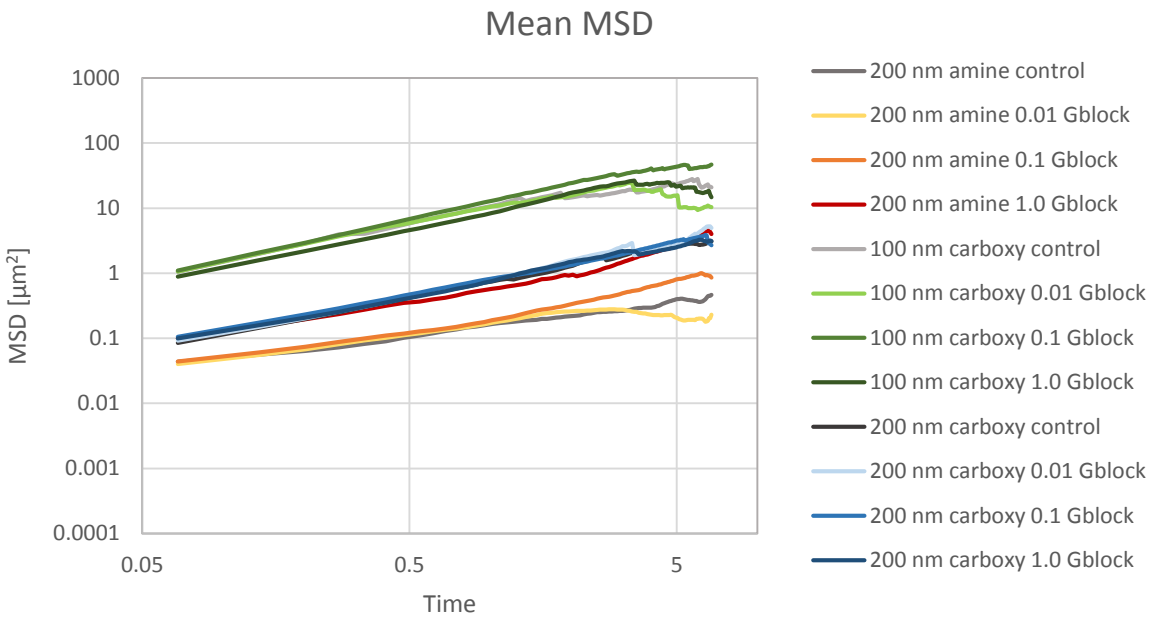


*Figure 4.5.3: Graph of mean MSD values of all the trajectories from the graphs A to H in Figure 4.5.1 and A to D in Figure 4.5.2. The nanoparticles are 200 nm aminated or 100 or 200 nm carboxylated particles in PSIM with added G-block in three different concentrations (0.01, 0.1 and 1.0 mg/mL) and a control with physiological saline.*

Figure 4.5.3 shows an overview of the mean value MSD trajectories from Figure 4.5.1 and 4.5.2. The results show that the 100 nm carboxylated particles are the most mobile, and the 200 nm aminated particles are the least mobile, with the 200 nm carboxylated particles somewhere in between. There is no visible effect of the addition of G-blocks.

However, because of the observation stated above about the carboxylated particles having two subpopulations, a graph of mean MSD values is a poor representation of the information obtained. This can be seen for the 100 and 200 nm carboxylated nanoparticles in Figure 4.5.1. MSD distribution graphs were therefore made to be able to properly view and assess the information in the data.

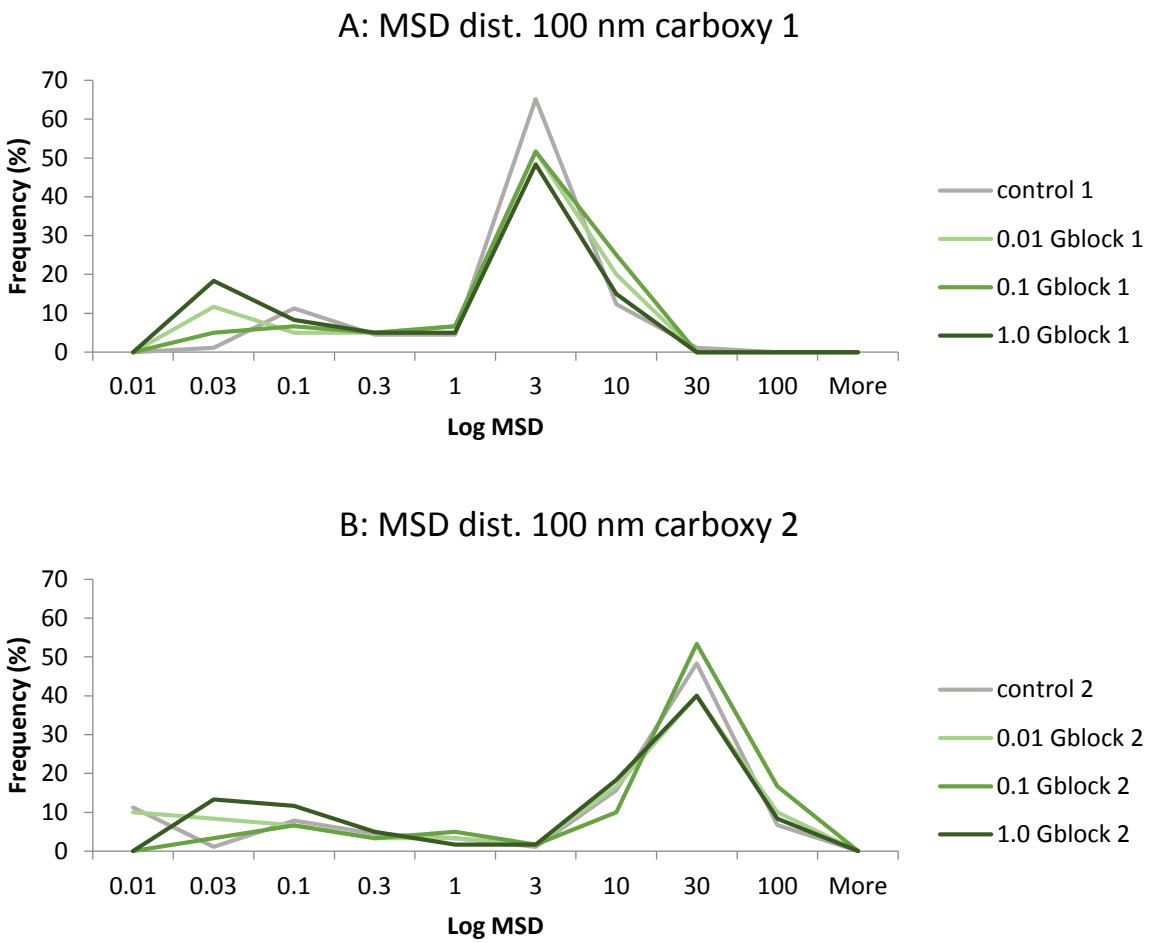


*Figure 4.5.4: Graphs of MSD distribution at two points of time scale (1: 0.136 and 2: 1.3604) for 100 nm carboxylated nanoparticles in PSIM with added G-block in three different concentrations (0.01, 0.1 and 1.0 mg/mL) and a control with physiological saline.*

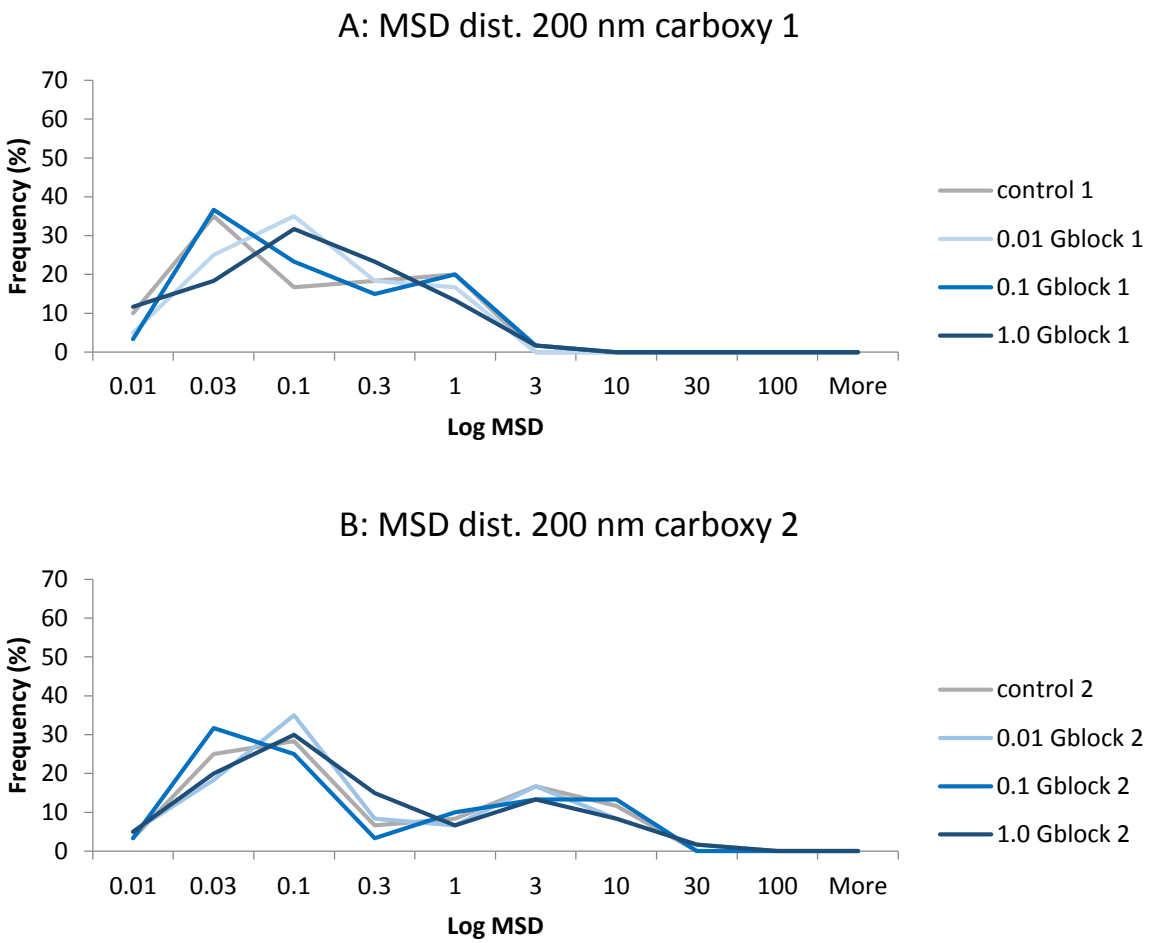


*Figure 4.5.5: Graphs of MSD distribution at two points of time scale (1: 0.136 and 2: 1.3604) for 200 nm carboxylated nanoparticles in PSIM with added G-block in three different concentrations (0.01, 0.1 and 1.0 mg/mL) and a control with physiological saline.*

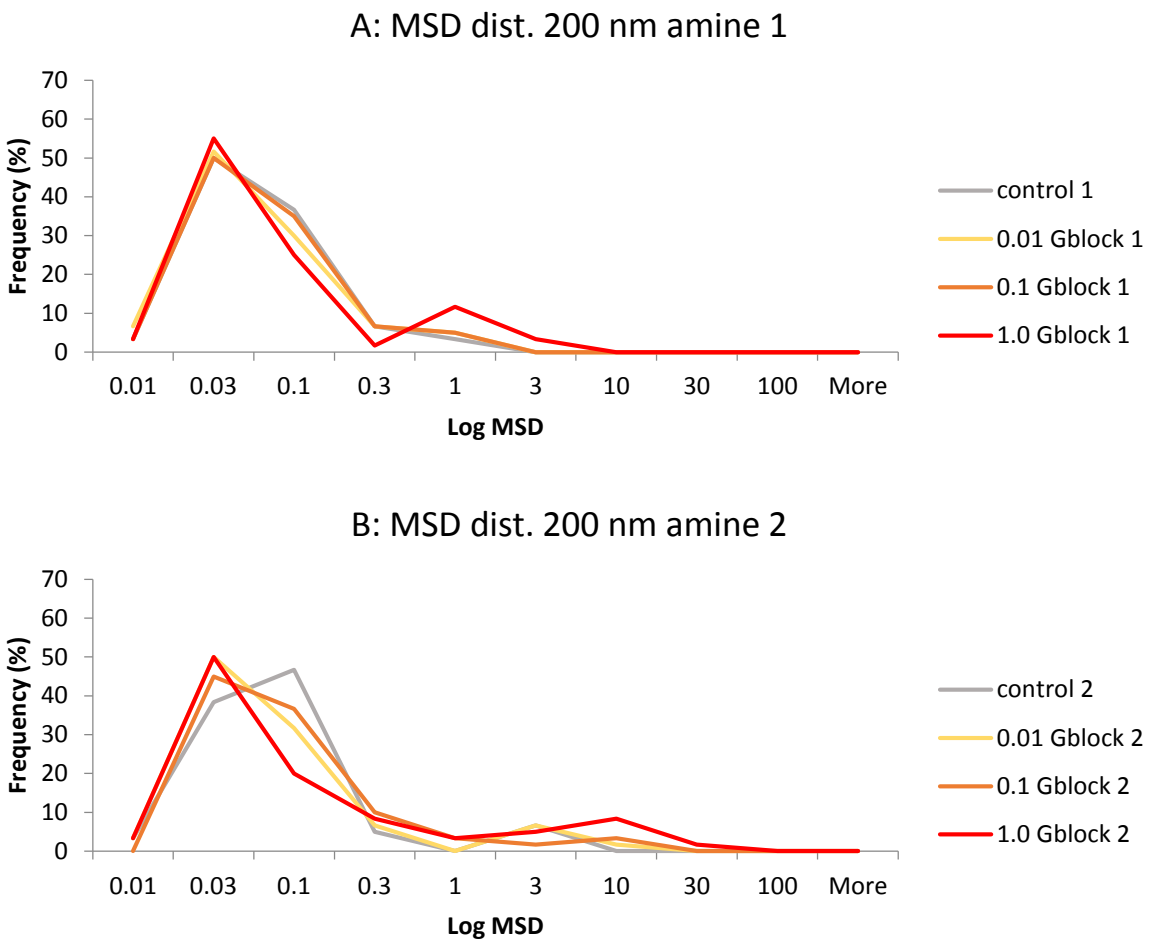


*Figure 4.5.6: Graphs of MSD distribution at two points of time scale (1: 0.136 and 2: 1.3604) for 200 nm aminated nanoparticles in PSIM with added G-block in three different concentrations (0.01, 0.1 and 1.0 mg/mL) and a control with physiological saline.*

As can be seen from the Figures 4.5.4-4.5.6, the 200 nm aminated and 100 and 200 nm carboxylated particles in PSIM with added G-blocks are indeed divided into two subpopulations. The 100 nm carboxylated particles (Figure 4.5.4) have a large mobile and a small immobile subpopulation. The 200 nm carboxylated particles (Figure 4.5.5) have a medium sized immobile subpopulation and a bit smaller and slightly more mobile subpopulation. The 200 nm aminated particles (Figure 4.5.6) have a large immobile and a small mobile subpopulation. The intensity of the colours signify the concentration of G-blocks added, with grey being no G-block, pale colour is 0.01, intermediate is 0.1, and dark is 1.0 mg/mL added G-blocks. There seems to be no consistent effect of the G-blocks.

## 4.6 Comparison of overall particle mobility in biosimilar mucus and PSIM

For comparison reasons, an examination of 200 nm aminated and 100 and 200 nm carboxylated nanoparticle mobility in biosimilar mucus was performed. This experiment would allow evaluation of differences in particle mobility between biosimilar mucus and PSIM for even more particle types. The results are shown in Figure 4.6.1, and an overview of the mean MSD value graphs are found in Figure 4.6.2.

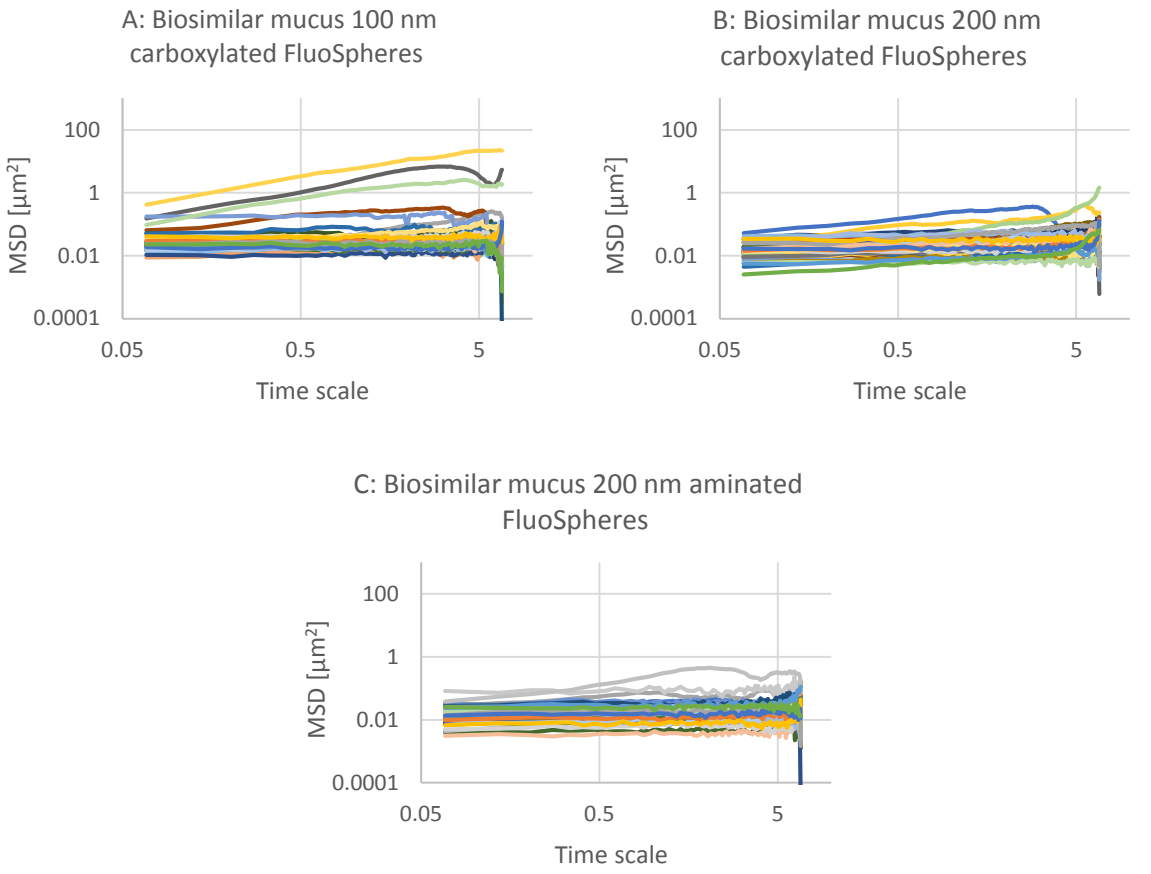


*Figure 4.6.1: Graphs A to C of MSD values for 100 and 200 nm carboxylated particles and 200 nm aminated particles in biosimilar mucus. The number of trajectories in each graph is about 60. Referring to Table 3.4.1, the wells corresponding to the letters are A-2, B-3, C-6.*

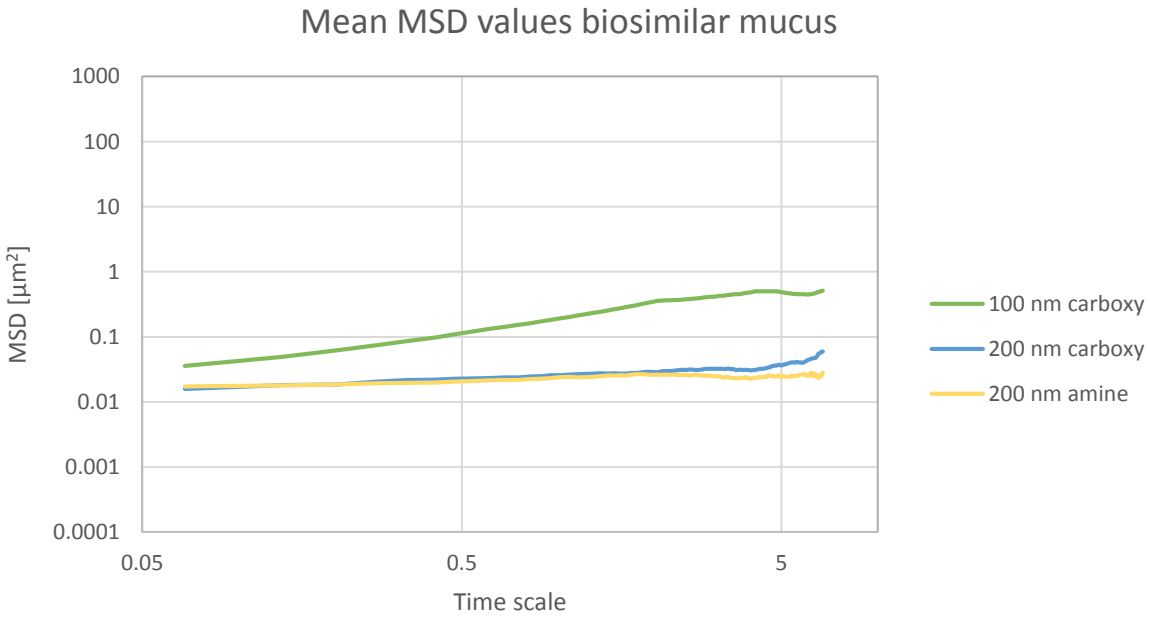


*Figure 4.6.2: Graph of mean MSD values for 100 and 200 nm carboxylated particles and 200 nm aminated particles in biosimilar mucus. Graphs of all the trajectories can be found in Figure 4.6.1, graphs A to C.*

Figure 4.6.2 shows that all three of the tested particles are stationary in the biosimilar mucus, with the 100 nm carboxylated particles being slightly more mobile than the 200 nm carboxylated and aminated particles.

By taking the mean MSD data from Figure 4.6.2 and combining it with mean MSD mobility data for 200 nm aminated and 100 and 200 nm carboxylated particles in PSIM (Figure 4.5.3), and mean MSD mobility data for 100 nm aminated and 200 nm PEGylated particles in biosimilar mucus (Figure 4.3.2) and PSIM (Figure 4.3.4), a comprehensive overview of the differences in particle mobility between biosimilar mucus and PSIM is produced, which can be seen in Figure 4.6.3 and Figure 4.6.4.

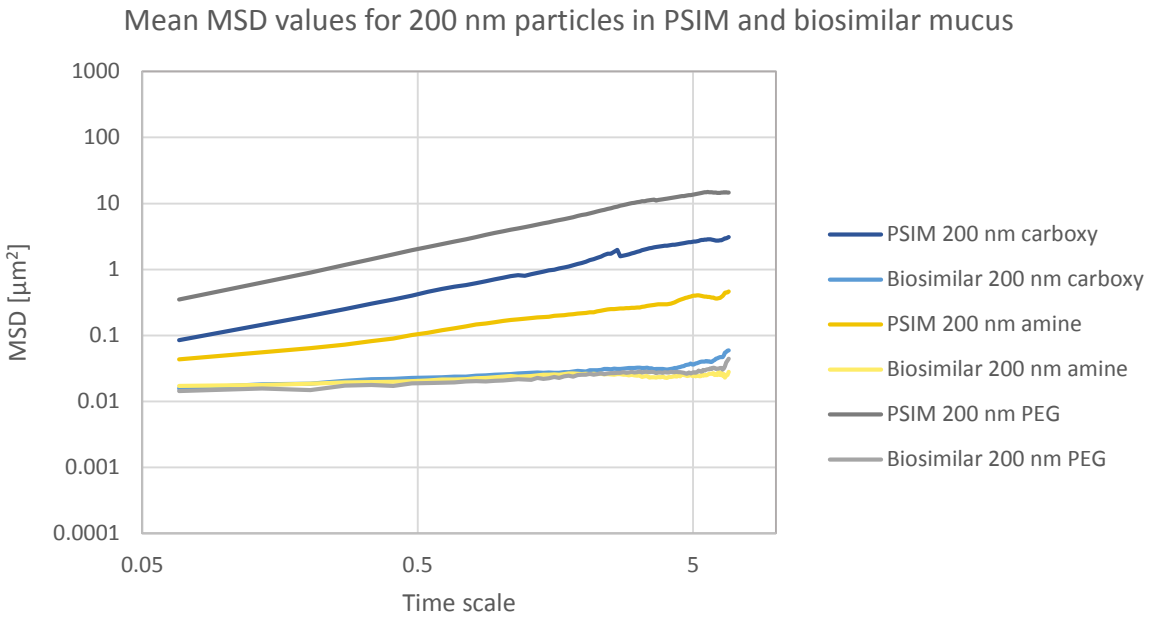


*Figure 4.6.3: Graph of mean MSD values for 200 nm carboxylated, aminated and PEGylated particles in biosimilar mucus and PSIM.*

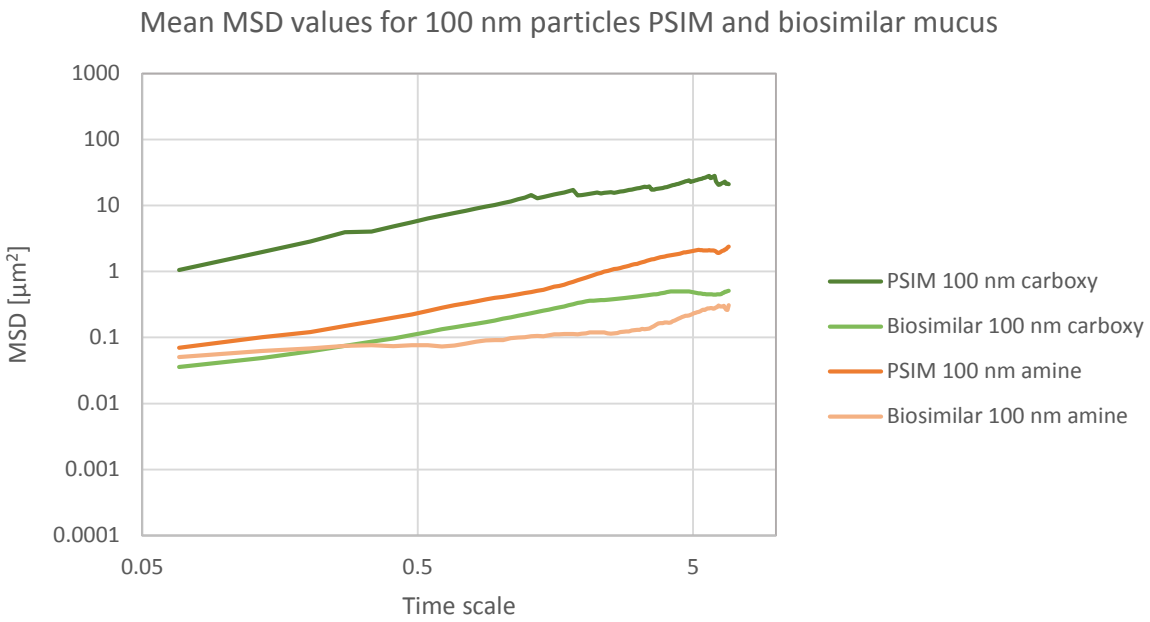


*Figure 4.6.4: Graph of mean MSD values for 100 nm carboxylated and aminated particles in biosimilar mucus and PSIM.*

In Figure 4.6.3 and Figure 4.6.4, the same type of particle has the same colour. The pale colours signify particles in biosimilar mucus, while the darker colours signify particles in PSIM. For example, the pale blue trajectory is the mean MSD values for 200 nm carboxylated particles is biosimilar mucus, while the dark blue trajectory is mean MSD data for the same particle in PSIM. The results show that, for the five particles that were tested, all of the trajectories in PSIM are above the corresponding trajectories in biosimilar mucus. This means that each particle is markedly more mobile in PSIM compared to the same particle in biosimilar mucus. There are some differences between the particles. For the 100 nm and 200 nm aminated particles the difference in mobility between the two types of mucus is not that great, while for the 200 nm PEGylated particles the difference in mobility is huge.

During the project work, different of particles were examined and a large amount of particle mobility data was collected. An unexpectedly large difference in particle mobility between biosimilar mucus and PSIM (porcine small intestinal mucus) was observed already after the first experiments (Figure 4.2.2), and this was something that was early on decided to investigate further. A comprehensive overview of the differences in particle mobility between biosimilar mucus and PSIM can be seen in Figure 4.6.3 and Figure 4.6.4. By comparing the mean MSD trajectories of nanoparticles in biosimilar mucus (pale colours) with the same type of data in PSIM (dark colours), it becomes obvious that there is a significant change in particle mobility for the two types of mucus. The mobility of the particles measured in the biosimilar mucus is consistently lower than the mobility of the same particles recorded in PSIM. The difference is particularly high for the more mobile particles, like the 100 nm carboxylated and especially the 200 nm PEGylated particles. However, even the less mobile types, like the 200 nm aminated particles, have a markedly higher mobility in the PSIM. Thus, the results from the comparison of nanoparticle mobility in biosimilar and intestinal mucus suggest that biosimilar mucus may not be a good model for the transport of particles in small intestinal mucus.

# 5. Discussion

## 5.1 The effect of size and surface modification on particle mobility in PSIM

The particles initially compared were 200 nm PEGylated and 100 nm aminated particles. These particles were chosen to represent the extremes in mobility and immobility. It has been reported that 100 nm aminated particles are stationary (PSIM and porcine tracheal respiratory mucus) (Crater and Carrier 2010, Yang *et al.* 2012), and in contrast the 200 nm PEGylated particles are reported to be mobile (human cervicovaginal mucus) (Lai *et al.* 2009a). This is because the positive charges of the aminated particles cause them to interact with the negatively charged regions of the mucins and become stationary. In addition, these particles are small enough (100 nm) to enter small pores in the mucus network and become stuck. Entering the pores in the mucus network would also allow the particles to be exposed to more potential interaction sites. The PEGylated particles are larger and are excluded from the small pores. They are in theory neutral, but are hydrophilic and have on average a slight negative charge. Thus, they should be less affected by electrostatic interactions and quite mobile in intestinal mucus. However, these might not have been the optimal particles for comparison of size and mobility, since they differ in both size and surface modification, but this was not the aim of the project. Thus, both of these variables have to be taken into account when interpreting the data. When assessing the effect of particle size on mobility, the particles should ideally be of the same type to eliminate other variables. When comparing the 100 and 200 nm carboxylated/aminated nanoparticles, it is obvious from Figure 4.6.3 and Figure 4.6.4 that the smaller particles are more mobile than the larger particles of the same type. This is in agreement with results obtained during earlier studies of particle mobility in CF sputum, where 100 nm, 200 nm and 500 nm carboxylated particles had high, intermediate and low mobility, respectively (Dawson *et al.* 2003). However, other studies have reported 100 nm carboxylated and PEGylated particles as less mobile compared to 200 nm and 500 nm particles with identical surface modifications in human cervicovaginal mucus (Lai *et al.* 2009a). Thus, there seems to be some contradicting reports regarding this. This could be attributed to the fact that each of these studies makes use of different mucus models, and that mucus composition and structure differ between species, individuals and excretion sites. The various types of mucus will have different properties and it would be expected that particle mobility could be different in each mucus matrix.

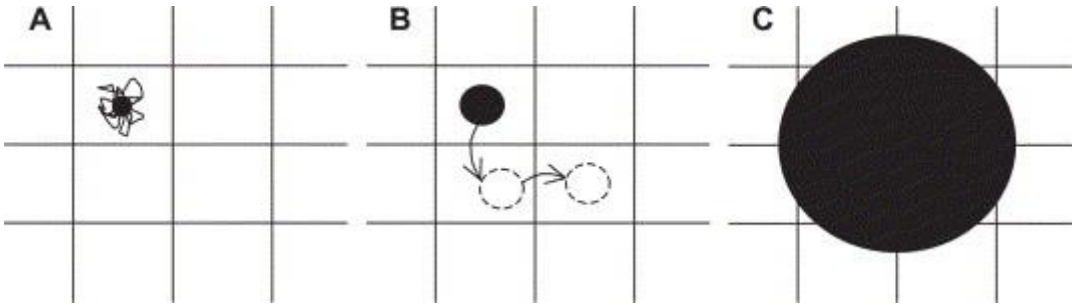


*Figure 5.1.1: Different scales of transport in complex environments. A: microscopic, B: mesoscopic and C: macroscopic transport (Suh et al. 2005).*

The mobility of particles in a complex environment like the mucus matrix can be very different depending on the size, as shown in Figure 5.1.1. The figure shows different transport modes in mucus, which are micro-, meso- and macroscopic transport. Microscopic transport is unobstructed short range Brownian motion, observed when the particle is small compared to the mucus pores. Mesoscopic transport will cause the particle to display an apparent caged motion on lower time scales and more diffusive motion on longer time scales, and is observed when the particle size approaches the pore size of the mucus. Macroscopic transport occurs when the particle is markedly

larger than the pore size, and the particles will display a more homogeneous diffusion (Suh *et al.* 2005). A particle of any size can undergo all of these transport modes in mucus, as mucus pore size is heterogeneous. The mobility of particles undergoing macroscopic transport will be observed as being slower than the mobility of particles undergoing microscopic transport, because of the varying degrees of steric hindrance. However, this view only focuses on size and disregards the effect of particle-mucus interactions (Suh *et al.* 2005). In general, the particles that were examined during the project have varying mobility within the same type of particles in the same type of mucus medium. This is a behaviour commonly seen when particles are submerged in a heterogeneous medium (Crater and Carrier 2010). A heterogeneous medium such as native mucus will have large differences in pore sizes. Particles will move slowly through smaller pores and more quickly through larger pores, causing the heterogeneity in particle velocity seen in the results (Dawson *et al.* 2003). A more uniform distribution of particle velocities could be caused by a more homogeneous medium, as this would cause the particles to follow a limited number of paths. These few paths would be where the pore sizes are big enough for the particles to move through and the particles would thus show less diversity of movement (Dawson *et al.* 2003). While the results with PSIM show some heterogeneity in particle mobility, the results with biosimilar mucus are much less diverse. A possible explanation could be that the pore sizes in biosimilar mucus are on average smaller than in PSIM, and this is discussed in greater detail in section 5.2. However, this interpretation assumes no interaction between the particle and the mucus, and mucus-particle interactions could give a different result.

To compare the effect of surface modification on particle mobility, one would use same size nanoparticles of different types. The aminated particles have a positive charge, the carboxylated particles have a negative charge, and the PEGylated particles have an almost neutral, slightly negative charge and a hydrophilic surface. From Figure 4.6.3 and 4.6.4 it is clear that the carboxylated particles are more mobile than the aminated particles, for both the 100 nm and 200 nm sized particles. The difference in mobility seems to be larger for the smaller particles. This could be explained by the larger particles having a larger surface area. They might therefore be more affected by surface interactions compared to the smaller particles, who have a smaller surface area. This would cause the larger particles to be less mobile compared to the smaller particles. The 200 nm particles would then have a smaller relative difference in mobility between the carboxylated and aminated particles.

The positive charges of the amine groups on the aminated particles will interact with the negatively charged parts of the mucin network through electrostatic interactions, while the carboxylated particles will interact with the positively charged parts of the mucin network, for example positively charged amino acids. The observed results could be partly explained by the overall higher frequency of negative charges on the mucin molecules in comparison with positive charges. Thus, the aminated particles will be more hindered by electrostatic attraction to the mucins in comparison with the carboxylated particles, while the PEGylated particles will have little electrostatic interactions. All three types of particles, both aminated, carboxylated and PEGylated, contain hydrogen atoms bound to an electronegative atom (O, N) and can interact with nearby molecules through hydrogen bonding. The amount of electrostatic interactions and, to a substantially lesser degree, hydrogen bonding will be pH dependent, as the pH will affect the protonated or deprotonated status of the carboxyl and amino groups. All of the particles also have a hydrophobic core because of the polystyrene material, and could in theory undergo hydrophobic interactions with other molecules. The degree of hydrophobic interaction will be dependent on how dense the surface coating of the particles are. Considering the high degree of surface coating for the particles in question, it is reasonable to assume that hydrophobic interactions will not be the dominant type of interaction. Especially the PEGylated particles will likely not undergo hydrophobic interactions because of the

increased spacing caused by the coating with PEG, which will probably sufficiently mask the hydrophobic core. In addition to interacting with the mucus network, the particles could also interact with the other compounds present, like other proteins, ions and lipids. The particles will probably exhibit all of the three types of interactions described to some degree.

Overall, larger particles (500 nm and up) are found to be immobile in mucus networks (Dawson *et al.* 2003, Lai *et al.* 2009a, Schuster *et al.* 2013, Yang *et al.* 2012). Aminated particles are generally reported as immobile, including small particles (Crater and Carrier 2010, Yang *et al.* 2012), though they were reported as mobile in CF sputum (Dawson *et al.* 2003). PEGylated particles are generally reported as mobile, when they are under a certain size limit (500 nm) (Lai *et al.* 2009a, Lai *et al.* 2011, Schuster *et al.* 2013, Yang *et al.* 2012). Subpopulations of outlier 100 nm and 200 nm PEGylated particles with high mobility have been reported as especially interesting because they are able to penetrate deep into mucus layers (Lai *et al.* 2011). Carboxylated particles have varying results, with some saying they are immobile, others reporting, mobile or intermediate, and yet others reporting subpopulations where some particles are mobile and some are immobile (Dawson *et al.* 2003, Nordgård *et al.* 2014, Lai *et al.* 2009a, Schuster *et al.* 2013). The mucus models used in the above examples are PSIM (Crater and Carrier 2010), CF sputum (Dawson *et al.* 2003), porcine gastric mucus (Nordgård *et al.* 2014), human cervicovaginal mucus (Lai *et al.* 2009a), human chronic rhinosinusitis mucus (Lai *et al.* 2011), human respiratory mucus (Schuster *et al.* 2013), and porcine tracheal respiratory mucus (Yang *et al.* 2012).

## 5.2 Comparison of biosimilar mucus and small intestinal mucus

Biosimilar mucus, as mentioned, was developed as a biocompatible alternative for biological intestinal mucus, and it was supposed to be model for the rheological and barrier properties for compound diffusion in porcine intestinal mucus. Because of this, one could expect that the behaviour of the nanoparticles in biosimilar mucus would be similar to their behaviour in small intestinal mucus. As shown in the results from the comparison of particle mobility in biosimilar mucus and small intestinal mucus, notably Figure 4.6.3 and Figure 4.6.4, this is not the case.

The results from the comparison of nanoparticle mobility in biosimilar and intestinal mucus suggest that biosimilar mucus may not be a good model for the transport of particles in small intestinal mucus. As described in section 1.6, the rheological and barrier properties of biosimilar mucus was originally tested by the creators, and found to be comparable to those of small intestinal mucus. The compounds used in the test for barrier and transport properties were representative of both hydrophobic and hydrophilic compound, but they were all small molecules (Boegh *et al.* 2014). The behaviour of small molecules in mucus is likely to be very different from the behaviour of larger compounds like nanoparticles and biologicals, since small molecules can diffuse much more easily through the mucus and avoid being trapped by the steric barrier posed by the mucin network (Olmsted *et al.* 2001).

The varying mobility of the particles that were examined is common when particles are submerged in a heterogeneous medium because of the varying pore sizes (Crater and Carrier 2010). By comparing Figure 4.3.1 and 4.3.3 it is apparent that the particle mobility in PSIM show more variance than the same particles in biosimilar mucus. An explanation to this result could be that the biosimilar mucus does not contain the same variance in pore sizes that is commonly seen in native mucus. Less variety in pore sizes could cause a more uniform distribution of particle velocities. This could be caused by the differences in composition between PSIM and biosimilar mucus, discussed in more detail below. This more homogeneous pore size distribution could explain the lower variation in particle mobility in biosimilar mucus. Alternatively, the pores of the biosimilar mucus could be very

small compared to the particles, as this would cause the particles to follow a limited number of paths, and the particles would thus show less diversity of movement (Dawson *et al.* 2003). As mentioned, this theory does not take particle interaction into consideration, and interaction between the particle and the mucus components could affect particle behaviour.

Other researchers have confirmed the rheological similarities between biosimilar mucus and PSIM and concluded that it would likely be a good model system for drug absorption testing (Våset 2014). However, according to the results produced in this study, this does not appear to hold true for drugs with sizes in the nanometre range. Rheological measurements of biosimilar mucus with added G-blocks of different molecular weights have also been performed (Reehorst 2014). The results showed that the addition of $DP_n$ 12 G-block had no effect on the structure of the biosimilar mucus, while the addition of $DP_n$ 33 G-block caused a weakening of the biosimilar mucus network. This could be an explanation as to why no effect of G-blocks was observed in biosimilar mucus during this project, as the G-blocks that were used had a $DP_n$ of 12. However, the mechanism proposed for this interaction between G-blocks and biosimilar mucus was a phase separation mechanism, not electrostatic interactions as in PSIM. In the same experiment, $DP_n$ 12 G-blocks were shown to weaken the PSIM network. Earlier studies have shown that G-blocks of low molecular weight ($DP_n$ 10 and $DP_n$ 20) have a weakening effect on porcine gastric mucin gels, PSIM and human cystic fibrosis sputum (Draget 2011, Draget and Taylor 2011, Nordgård and Draget 2011, Nordgård *et al.* 2014, Taylor *et al.* 2007). Even though the results obtained in this study do not appear to agree with these earlier reports, it is likely to assume that the interaction between the G-blocks and the biosimilar mucus must differ from native mucus. This can be explained by examining the differences in biosimilar mucus and native mucus content. Biosimilar mucus is, as described in section 3.3, prepared with Sigma mucin, which is a rough mixture of mucin glycoproteins, and it is "obtained by digestion of hog stomach with pepsin, followed by precipitation and other steps (Sigma-Aldrich 2011)." This Sigma mucin has been altered and probably partly fragmented by the processes it went through as it was isolated, particularly the digestion with pepsin. Thus, it differs in structure from the mucins found in native mucus like PSIM (Kočevar-Nared *et al.* 1997). As described in section 1.2.1, mucins found in native mucus are of high molecular weight with a high number of weak bonds and interactions between them, and this structure could easily be altered by fragmentation. In addition, biosimilar mucus contains polyacrylic acid (PAA), which is not found in native mucus, but was added by the creators to achieve the desired rheological properties (Boegh *et al.* 2013, Boegh *et al.* 2014). The addition of the PAA alters the structure of the mucins for the biosimilar mucus to achieve viscoelastic properties similar to PSIM, but might also interfere with the effect of G-blocks on the mucins. Earlier reports have stated that non-mucin components can contribute to weaken a mucus gel, because they interrupt mucin associations (Bell *et al.* 1985).

## 5.3 The effect of added G-blocks to particle mobility in PSIM

The aim of the project was to investigate whether G-blocks can improve the mucomobility of PEGylated nanoparticles. The effect of G-blocks on 200 nm PEGylated particles in PSIM can be seen in Figure 4.3.4 and Figure 4.4.2. Adding G-block does not seem to have a significant effect on 200 nm PEGylated nanoparticles. A possible explanation could be that the G-blocks only affect particles who have an initially poor mobility. Since the mobility of the PEGylated particles is already high, adding G-blocks produces no measurable results. However, since other less mobile particles show little improvement in mobility from added G-blocks, this is likely not the only cause.

Figure 4.5.3 also shows mean MSD mobility data for 100 and 200 nm carboxylated particles in PSIM with added G-blocks. From this figure, no effect of G-blocks on the particles can be seen. However, since these particles seemed to have two subpopulations, MSD distribution graphs were made to

better evaluate the information in the data, and these can be seen in Figures 4.5.4-4.5.5. These figures are somewhat hard to analyse, but there does not appear to be any consistent effect of the added G-blocks.

Figure 4.3.4 and Figure 4.4.2 also show the effect of G-block on 100 nm and 200 nm aminated particles, respectively. While the 100 nm aminated particles in Figure 4.3.4 show no definite pattern with increasing G-block concentration, the 200 nm aminated particles in Figure 4.4.2 seem to be more mobile with increasing G-block concentration. Figure 4.5.3 also shows the effect of G-block on 200 nm aminated particles, but in this case only the highest concentration of G-blocks had an increased mobility in comparison with the control sample. The corresponding MSD distribution graph (Figure 4.5.6) shows that the highest concentration of G-blocks have caused an increase in the mobile subpopulation of the 200 nm aminated particles and a decrease in the amount of slightly mobile particles, while the size of the completely stationary subpopulation is unchanged. This suggests that the G-blocks cannot affect the mobility of particles who are tightly bound to the mucus network. It is also possible that adding G-blocks to mucus can affect the pores of various sizes in different ways. One study hypothesised that the addition of $DP_n$ 12 and $DP_n$ 33 G-blocks to a PG mucin gel caused both an opening of the smaller pores in the mucin network, but also a decrease in the larger pores. It was theorised that this was due to G-block-mucin interactions (Reehorst 2014). However, as previously discussed, mucin gels and native mucus are inherently different, so this information might not be comparable. The mucin gel used in this study was not prepared with Sigma mucin and would not have the same problems with degraded Sigma mucin molecules, but natural mucus still exhibit a higher complexity in components and structure compared to a mucin-only gel.

Earlier studies have shown that G-blocks of low molecular weight ($DP_n$ 10 and $DP_n$ 20) have a weakening effect on porcine gastric mucin gels, PSIM and human cystic fibrosis sputum (Draget 2011, Draget and Taylor 2011, Nordgård and Draget 2011, Nordgård *et al.* 2014, Taylor *et al*. 2007). Another study showed that G-blocks with $DP_n$ 12 weakened the PSIM network (Reehorst 2014). As mentioned in section 1.5, the mechanism for G-block interaction with mucus has been suggested to be by electrostatic interaction. The positively charged regions of the mucin molecules, caused by positive amino acids, is a potential interaction site for the negatively charged G-blocks, in addition to being a site for intermucin and intramucin interaction (Nordgård and Draget 2011). Adding G-blocks was expected to change these interactions by interfering with the mucin structure by electrostatic interactions and reducing the crosslinks between mucins and other mucus components, thereby weakening the mucus gel structure and causing an increased particle mobility. All of the particles, both aminated, carboxylated and PEGylated will, as described, probably exhibit both hydrogen bonding, and hydrophobic and electrostatic interactions. Adding G-blocks could also be theorised to possibly hide potential particle-mucin binding sites, again leading to higher mobility. This would be expected to influence the negatively charged particles to a larger degree, since the G-blocks have a negative charge and would be attracted to the positively charged regions of the mucin molecules, hindering these regions from interacting with the negative particles.

In contrast to earlier studies, the results obtained here do not show any consistent effect of adding G-blocks to improve the mucomobility of nanoparticles. One possible explanation is that the PSIM used in this study was somehow different from the native mucus used in the earlier studies. The PSIM used in the preparation of the samples came from the same batch, which was originally obtained about 18 months earlier. The PSIM was frozen at -20 °C in a number of beakers. The beakers with PSIM were in use by other students or researchers and it is likely that some of them have been thawed and refrozen numerous times. It is possible that repeated freezing have affected the structure and properties of the native mucus. Previous research on the effect of freezing on

different types of mucus have shown varying results, as both significant effects and no significant effects on the viscoelastic properties of frozen mucus samples have been reported (Sanders *et al.* 2000, Boegh *et al.* 2013, Boegh *et al.* 2014, Groo and Lagarce 2014). However, it is uncertain what effect many repeated rounds of thawing and freezing could have on mucus. It could be theorised that repeated thawing and freezing causes a weakening of the mucus structure, for example by ice crystal formation, and that an already weakened mucus gel would show no further effect from the addition of G-blocks. One could also argue against this theory by pointing out that if that was the case, the mobility of the particles, especially the less mobile ones, should have been higher than expected because of the weakened structure. However, this is not certain since a weakened mucus gel structure could also cause a collapse of the mucus pores, leading to a more hindered particle mobility because of the increased steric hindrance.

Though unlikely, it cannot be completely excluded that earlier studies might have overestimated the effects of G-blocks in weakening mucus. However, this seems very improbable because of the sheer number of results that demonstrate and verify the effects of G-blocks. In addition, both several different methods and mucus models are used, which all support the previous statement. The MUCOVA G-block technology is currently in phase two of clinical trials, with results showing a decreased viscosity of CF sputum after treatment (personal communication, Kurt I. Draget).

Another thing that becomes apparent when comparing the results from the two experiments with 200 nm aminated particles and added G-blocks (Figure 4.4.2 and Figure 4.5.3) is that the overall mobility of the particles in the later experiment is markedly higher than what was found in the previous experiment. This could be explained by the natural diversity of the mucus content and structure. Native mucus has a high degree of natural variety in content and thus in structure and expressed properties, as it contains both diverse mucins and other proteins in addition to lipids, ions and other substances (Bansil and Turner 2006, Boegh *et al.* 2014). The mucus used in the experiments was stirred after thawing to reduce heterogeneity. However, while the PSIM used in the preparation of the samples came from the same batch, they were frozen in a number of beakers, and there is no guarantee that the same beaker was used for preparation of each of the different experiments. In addition, as mentioned above, the PSIM could have been thawed and frozen a number of times, which could possibly have affected the structure of the mucus. This could have contributed to the high degree of variation in particle mobility that was observed.

## 5.4 Evaluation of method

MPT is a non-invasive and highly selective and sensitive method for assessing individual nanoparticle mobility. It is also non-destructive, and is well suited to give a measure of the heterogeneity of the mucus network and pore size (Dawson *et al.* 2003). It can be used to quantify the amount of adherent and mobile particles, and give a measure of how hindered the particles are by the mucus layer (Lai *et al.* 2009a).

A possible problem with the MPT method is the particle selection bias of the researcher during particle tracking with Speckle Tracker. Since each particle to be tracked is manually chosen by the researcher, it is important to be aware of the big impacts any eventual bias towards more or less mobile particles can have on the results. Care must therefore be taken to choose the particles to be tracked randomly and without bias. Other programs can automatically select and track particles, eliminating this problem. However, these programs can give problems since they might automatically detect various undesirable items.

As explained in section 1.6, the MPT technique is prone to imprecisions in MSD values at lengthy time scales, causing noise in the graphs depicting the MSD values (Saxton and Jacobson 1997). This is

because of the way the MSD values are calculated by taking the means of a number of displacement values. At short time scales the MSD values are the means of a large number of displacement values, but the number of displacement values used to calculate the MSD values is reduced as the time scale increases. The last MSD value at the longest time scale consists of just one displacement value. Thus, the MSD values at larger time scales are less statistically accurate (Saxton and Jacobson 1997, Suh *et al.* 2005). Some noise can be seen in the results obtained, for example in Figure 4.3.3, but large amounts of noise has overall not been a problem in this study.

Care must be taken when tracking particles using MTP to ensure that the particles are not simply floating with the motion of the mucus medium (Suh *et al.* 2005). The particles could be moved around by the movements of the mucus, instead of moving on their own. The mucus medium might be set in motion by the lateral movement of the sample during examination and filming with the confocal microscope. The videos were therefore examined before analysis to ensure that the particles were moving independently and not in the same direction. By examining an xy-plot of the measured particles, one can see that they are clearly moving independently which eliminates this possible error (data not included). Another thing to keep in mind is that the intense light from the confocal microscope will heat the examined sample over time, and this could possibly have an effect on the structure and stability of the mucus or nanoparticles. This did not likely have a big influence on the results because the samples were not exposed to heat for long measures of time, and the samples were also covered, so evaporation of water was minimized.

An alternative method to examine the mobility of particles is fluorescence recovery after photobleaching (FRAP). This technique uses photobleaching of an area and monitoring of the recovery of the fluorescent particles to measure the ability of the molecules to move around over time. Very mobile particles will result in a rapid recovery of the fluorescence to the bleached area, while immobile particles will result in little or no recovery of fluorescence. However, FRAP is often used with a large concentration of particles, since a big difference between the fluorescence levels before and after photobleaching is preferred. Also, this method would not pick up on small variances in mobility, like for example particles vibrating in place, or particles moving around but not covering any significant distance. In addition, FRAP will only give information about average diffusion rates and might miss information about multiple subpopulations or heterogeneity in individual particle mobility, which is to be expected from a heterogeneous network such as the one found in mucus (Lai *et al.* 2009a).

In contrast, the MPT method can pick up smaller variances in mobility, in addition to being able to obtain information on the single particle level. If a large number of particles are to be tracked, however, it could take a lot of time since each individual particle has to be selected, tracked, and the coordinate parameters analysed and converted to MSD values. Still, with the relatively low particle concentration and thus small amount of particles in this study, MPT was considered the best option for measuring mobility.

# 6. Conclusion and future work

During this study, the effect of G-blocks on nanoparticle mobility in biosimilar mucus and porcine small intestinal mucus was examined. Biosimilar mucus, as it is today, was found to not be a suitable model for the transport of large entities like nanoparticles in porcine small intestinal mucus, because of the large differences in particle mobility observed between the two types of mucus. However, changes in the composition of biosimilar mucus could possibly produce a more viable model.

There was no observed effect of adding G-blocks to increase particle mobility in porcine small intestinal mucus. This is in conflict with earlier reports. A possible explanation could be changes in mucus structure caused by repeated thawing and freezing.

To ascertain the results found during this study, future work could include duplicating the experiments. In addition, a study of the natural variety of native mucus would be interesting, in order to assess the effect of natural variation in mucus network composition and structure on the mobility of different nanoparticles.

# References


Bamrungsap, S.; Zhao, Z.; Chen, T.; Wang, L.; Li, C.; Fu, T.; Tan, W., *Nanotechnology in therapeutics: A focus on nanoparticles as a drug delivery system*. Nanomedicine **2012**, Vol. 7, Issue 8, *Pages 1253-1271*.

Bansil, R.; Turner, B. S., *Mucin structure, aggregation, physiological functions and biomedical applications*. Current Opinion in Colloid & Interface Science **2006**, Vol. 11, Issues 2-3, *Pages 164-170*.

Bell, A. E.; Sellers, L. A.; Allen, A.; Cunliffe, W. J.; Morris, E. R.; Ross-Murphy, S. B., *Properties of gastric and duodenal mucus: effect of proteolysis, disulfide reduction, bile, acid, ethanol, and hypertonicity on mucus gel structure*. Gastroenterology **1985**, Vol. 88, Issue 1, *Pages 269-280*.

Boegh, M.; Baldursdóttir, S. G.; Nielsen, M. H.; Müllertz, A.; Nielsen, H. M., *Development and Rheological Profiling of Biosimilar Mucus*. Annual Transactions of the Nordic Rheology Society **2013**, Vol. 21, *Pages 233-240*.

Boegh, M.; Baldursdóttir, S. G.; Müllertz, A.; Nielsen, H. M., *Property profiling of biosimilar mucus in a novel mucus-containing in vitro model for assessment of intestinal drug absorption*. European Journal of Pharmaceutics and Biopharmaceutics**. 2014**, Vol. 87, Issue 2, *Pages 227–235*.

Celli, J.; Gregor, B.; Turner, B.; Afdhal, N. H.; Bansil, R.; Erramilli, S., *Viscoelastic properties and dynamics of porcine gastric mucin*. Biomacromolecules **2005**, Vol. 6, Issue 3, *Pages 1329-1333*.

Chia-Ming, C.; Weiner, N., *Gastrointestinal uptake of liposomes. I. In vitro and in situ studies*. International journal of pharmaceutics **1987**, Vol. 37, Issues 1-2, *Pages 75-85*.

Cone, R. A., In: Mucosal Immunology, Second Edition, edited by Mestecky, Lamm, Strober, Bienenstock, and McGhee. Academic Press, San Diego **1999**. *Pages 43-66*.

Cone, R. A., *Chapter 4: Mucus*. In: Mucosal Immunology, Third Edition, edited by Mestecky, Lamm, Strober, Bienenstock, and McGhee. Academic Press, London **2005**. *Pages 49-72*.

Cone, R. A., *Barrier properties of mucus*. Advanced Drug Delivery Reviews **2009**, Vol. 61, Issue 2, *Pages 75–85*.

Crater, J. S.; Carrier, R. L., *Barrier Properties of Gastrointestinal Mucus to Nanoparticle Transport*. Macromolecular Bioscience **2010,** Vol. 10, Issue 12, *Pages 1473–1483*.

Cu, Y.; Saltzman, W. M., *Mathematical modeling of molecular diffusion through mucus*. Advanced drug delivery reviews **2009**, Vol. 61, Issue 2, *Pages 101-114*.

Dawson, M.; Wirtz, D.; Hanes, J., *Enhanced viscoelasticity of human cystic fibrotic sputum correlates with increasing microheterogeneity in particle transport*. Journal of Biological Chemistry **2003**, Vol. 278, Issue 50, *Pages 50393-50401*.

Draget, K. I., *Oligomers: Just background noise or as functional elements in structured biopolymer systems?* Food Hydrocolloids **2011**, Vol. 25, Issue 8, *Pages 1963-1965*.

Draget, K. I.; Nordgård, C. T., *MUCOVA: Drug delivery for large molecules and delivery vehicles*. NTNU, Technology Transfer Office (TTO) **2014**.

Draget, K. I.; Taylor, C., *Chemical, physical and biological properties of alginates and their biomedical implications*. Food Hydrocolloids **2011**, Vol. 25, Issue 2, *Pages 251-256*.

Ensign, L. M.; Cone, R.; Hanes, J., *Oral drug delivery with polymeric nanoparticles: The gastrointestinal mucus barriers*. Advanced Drug Delivery Reviews **2012**, Vol. 64, Issue 6, *Pages 557–570*.

Fellers, T. J.; Davidson, M. W., *Introduction to Confocal Microscopy*. Olympus Fluoview Resource Center, National High Magnetic Field Laboratory **2007**. Available at http://www.olympusconfocal.com/theory/confocalintro.html [accessed 09/05 2015].

Florence, A. T., *The oral absorption of micro-and nanoparticulates: neither exceptional nor unusual*. Pharmaceutical Research **1997**, Vol. 14, Issue 3, *Pages 259-266*.

Furrer, P.; Gurny, R., *Recent advances in confocal microscopy for studying drug delivery to the eye: Concepts and pharmaceutical applications*. European Journal of Pharmaceutics and Biopharmaceutics **2010**, Vol. 74, Issue 1, *Pages 33-40*.

Grazu, V.; Moros, M.; Sánchez-Espinel, C., *Nanocarriers as Nanomedicines: Design Concepts and Recent Advances*. Frontiers of Nanoscience **2012**, Vol. 4, *Pages 337-440*.

Groo, A.-C.; Lagarce, F., *Mucus models to evaluate nanomedicines for diffusion*. Drug Discovery Today **2014**, Vol. 19, Issue 8, *Pages 1097–1108*.

HUGO Gene Nomenclature Committee, *Gene Family: Mucins (MUC)*. European Bioinformatics Institute. Available at http://www.genenames.org/cgi-bin/genefamilies/set/648 [accessed 11/05 2015].

Kararli, T. T., *Comparison of the gastrointestinal anatomy, physiology, and biochemistry of humans and commonly used laboratory animals*. Biopharmaceutics and drug disposition **1995**, Vol. 16, Issue 5, *Pages 351-380*.

Khanvilkar, K.; Donovan, M. D.; Flanagan, D. R., *Drug transfer through mucus*. Advanced Drug Delivery Reviews **2001**, Vol. 48, Issues 2–3, *Pages 173–193*.

Kočevar-Nared, J.; Kristl, J.; Šmid-Korbar, J., *Comparative rheological investigation of crude gastric mucin and natural gastric mucus*. Biomaterials **1997**, Vol. 18, Issue 9, *Pages 677–681*.

Kornfeld, R.; Kornfeld, S., *Comparative aspects of glycoprotein structure*. Annual review of biochemistry **1976**, Vol. 45, Issue 1, *Pages 217-238*.

Kwon, K. C.; Verma, D.; Singh, N. D.; Herzog, R.; Daniell, H., *Oral delivery of human biopharmaceuticals, autoantigens and vaccine antigens bioencapsulated in plant cells*. Advanced drug delivery reviews **2013**, Vol. 65, Issue 6, *Pages 782-799*.

Lai, S. K.; Wang, Y.-Y.; Hanes, J., *Mucus-penetrating nanoparticles for drug and gene delivery to mucosal tissues*. Advanced Drug Delivery Reviews **2009** (a), Vol. 61, *Pages 158-171*.

Lai, S. K.; Wang, Y.-Y.; Wirtz, D.; Hanes, J., *Micro-and macrorheology of mucus*. Advanced drug delivery reviews **2009** (b), Vol. 61, Issue 2, *Pages 86-100*.

Lai, S. K.; Suk, J. S.; Pace, A., Wang, Y.-Y.; Yang, M.; Mert, O.; Chen, J.; Kim, J.; Hanes, J., *Drug carrier nanoparticles that penetrate human chronic rhinosinusitis mucus*. Biomaterials **2011**, Vol. 32, Issue 26, *Pages 6285–6290*.

Larhed, A.W.; Artursson, P.; Gråsjö, J.; Björk, E., *Diffusion of drugs in native and purified gastrointestinal mucus*. Journal of Pharmaceutical Sciences **1997**, Vol. 86, Issue 6, *Pages 660–665*.

Larhed, A. W.; Artursson, P.; Björk, E., *The Influence of Intestinal Mucus Components on the Diffusion of Drugs*. Pharmaceutical Research **1998**, Vol. 15, Issue 1, *Pages 66-71*.

Laroui, H.; Sitaraman, S. V.; Merlin, D., Chapter six – Gastrointestinal Delivery of Anti-inflammatory Nanoparticles. In: Methods in Enzymology Vol. 509, edited by Düzgüneş. Academic Press **2012**, *Pages 101–125*.

Lee, B. K.; Yun, Y. H.; Park, K., *Smart nanoparticles for drug delivery: Boundaries and opportunities*. Chemical Engineering Science **2015**, Vol. 125, *Pages 158–164*.

Lichtenberger, L. M., *The hydrophobic barrier properties of gastrointestinal mucus*. Annual review of physiology **1995**, Vol. 57, Issue 1, *Pages 565-583*.

McDonnell, T.; Ioannou, Y; Rahman, A., *PEGylated drugs in rheumatology—why develop them and do they work?* Rheumatology **2013**, Vol. 53, Issue 3, Pages *391-396*.

Nordgård, C. T.; Draget, K. I., *Oligosaccharides As Modulators of Rheology in Complex Mucous Systems*. Biomacromolecules **2011**, Vol. 12, Issue 8, *Pages 3084-3090*.

Nordgård, C. T.; Nonstad, U.; Olderøy, M. Ø.; Espevik, T.; Draget, K. I., *Alterations in Mucus Barrier Function and Matrix Structure Induced by Guluronate Oligomers*. Biomacromolecules **2014**, Vol. 15, *Pages 2294-2300*.

Norris, D. A.; Sinko, P. J., *Effect of size, surface charge, and hydrophobicity on the translocation of polystyrene microspheres through gastrointestinal mucin*. Journal of applied polymer science **1997**, Vol. 63, Issue 11, *Pages 1481-1492*.

Norris, D. A.; Puri, N.; Sinko, P. J.,*The effect of physical barriers and properties on the oral absorption of particulates.* Advanced drug delivery reviews **1998**, Vol. 34, Issue 2, *Pages 135-154*.

Olmsted, S. S.; Padgett, J. L.; Yudin, A. I.; Whaley, K. J.; Moench, T. R.; Cone, R. A., *Diffusion of macromolecules and virus-like particles in human cervical mucus*. Biophysical journal **2001**, Vol. 81, Issue 4, *Pages 1930-1937*.

Orive, G.; Gascon, A. R.; Hernández, R. M.; Domínguez-Gil, A.; Pedraz, J. L., *Techniques: new approaches to the delivery of biopharmaceuticals*. Trends in Pharmacological Sciences **2004**, Vol. 25, Issue 7, *Pages 382-387*.

Pawley, J. B., *Handbook of Biological Confocal Microscopy, Third Edition*. Springer Science + Business Media, New York **2006**.

Petros, R. A.; DeSimone, J. M., *+* Nature Reviews Drug Discovery **2010**, Vol. 9.

Ponchel, G.; Irache, J. M., *Specific and non-specific bioadhesive particulate systems for oral delivery to the gastrointestinal tract*. Advanced drug delivery reviews **1998**, Vol. 34, Issues 2-3, *Pages 191-219*.

Reehorst, C. M., *The mucin-alginate interplay: Investigating the rheological impact of alginates and their influence on particle mobility*. **2014.**

Rose, M. C.; Voynow, J. A., *Respiratory tract mucin genes and mucin glycoproteins in health and disease*. Physiological reviews **2006**, Vol. 86, Issue 1, *Pages 245-278*.

Rowland, R. N.; Woodley, J. F., *The stability of liposomes in vitro to pH, bile salts and pancreatic lipase.* Biochimica et Biophysica Acta (BBA)-Lipids and Lipid Metabolism **1980**, Vol. 620, Issue 3, *Pages 400-409*.

Sanders, N. N.; De Smedt, S. C.; Van Rompaey, E.; Simoens, P.; De Baets, F.; Demeester, J., *Cystic Fibrosis Sputum: a barrier to the transport of nanospheres*. American Journal of Respiratory and Critical Care Medicine **2000**, Vol. 162, Issue 5, *Pages 1905-1911*.

Sanders, N. N.; De Smedt, S. C.; Cheng, S. H.; Demeester, J., *Pegylated GL67 lipoplexes retain their gene transfection activity after exposure to components of CF mucus*. Gene Therapy **2002**, Vol. 9, Issue 6, *Pages 363-371*.

Sanders, N. N.; De Smedt, S. C.; Demeester, J., *Mobility and stability of gene complexes in biogels*. Journal of Controlled Release **2003**, Vol. 87, Issues 1–3, *Pages 117–129*.

Sanders, N.; Rudolph, C.; Braeckmans, K.; De Smedt, S. C.; Demeester, J., Extracellular barriers in respiratory gene therapy. Advanced drug delivery reviews **2009**, Vol. 61, Issue 2, Pages 115-127.

Savage, D. C., *Chapter 2 - Mucosal Microbiota*. In: Mucosal Immunology, Third Edition, edited by Mestecky, Lamm, Strober, Bienenstock, and McGhee. Academic Press, London **2005**. *Pages 19-33*.

Saxton, M. J.; Jacobson, K., *Single-particle tracking: Applications to membrane dynamics*. Annual Review of Biophysics and Biomolecular Structure **1997**, Vol. 26, *Pages 373-399*.

Schuster, B. S.; Suk, J. S.; Woodworth, G. F.; Hanes, J., *Nanoparticle diffusion in respiratory mucus from humans without lung disease*. Biomaterials **2013**, Vol. 34, Issue 13, *Pages 3439-3446*.

Sellers, L. A.; Allen, A.; Morris, E. R.; Ross-Murphy, S. B., *Mucus glycoprotein gels. Role of glycoprotein polymeric structure and carbohydrate side-chains in gel-formation*. Carbohydrate research, **1988**, Vol. 178, Issue 1, *Pages 93-110*.

Sellers, L. A.; Allen, A.; Morris, E. R.; Ross-Murphy, S. B., *The rheology of pig small intestinal and colonic mucus: weakening of gel structure by non-mucin components*. Biochimica et Biophysica Acta (BBA)-General Subjects **1991**, Vol. 1115, Issue 2, *Pages 174-179*.

Selvaggi, L.; Salemme, M.; Vaccaro, C.; Pesce, G.; Rusciano, G.; Sasso, A.; Campanella, C.; Carotenuto, R., *Multiple-particle-tracking to investigate viscoelastic properties in living cells*. Methods **2010**, Vol. 51, Issue 1, *Pages 20-26*.

Sheehan, J. K.; Kirkham, S.; Howard, M.; Woodman, P.; Kutay, S.; Brazeau, C.; Buckley, J.; Thornton, D. J., *Identification of molecular intermediates in the assembly pathway of the MUC5AC mucin*. Journal of Biological Chemistry **2004**, Vol. 279, Issue 15, *Pages 15698-15705*.

Shogren, R.; Gerken, T. A.; Jentoft, N., *Role of glycosylation on the conformation and chain dimensions of O-linked glycoproteins: light-scattering studies of ovine submaxillary mucin*. Biochemistry **1989**, Vol. 28, Issue 13, *Pages 5525-5536*.

Sigma-Aldrich, *Mucin from porcine stomach - M2378: FAQ*. Available at http://sigma-aldrich.custhelp.com/app/answers/list/p/7,984 [accessed 03/05 2015]

Smidsrød, O.; Moe, S. T., *Biopolymer chemistry*. Tapir Academic Press, Trondheim **2008**.

Strous, G. J.; Dekker, J., *Mucin-type glycoproteins*. Critical reviews in biochemistry and molecular biology **1992**, Vol. 27, Issues 1-2, *Pages 57-92*.

Suh, J.; Dawson, M.; Hanes, J., *Real-time multiple-particle tracking: applications to drug and gene delivery*. Advanced Drug Delivery Reviews **2005**, Vol. 57, Issue 10, *Page 1551*.

Suh, J., Choy, K.-L., Lai, S. K., Suk, J. S., Tang, B. C., Prabhu, S., & Hanes, J., *PEGylation of nanoparticles improves their cytoplasmic transport*. International Journal of Nanomedicine **2007**, Vol. 2, Issue 4, *Pages 735–741*.

Taylor, C.; Draget, K. I.; Smidsrød, O. A., *Use of oligouronates for treating mucus hyperviscosity*. Google Patents **2007**.

Thornton, D. J.; Sheehan, J. K., *From mucins to mucus: toward a more coherent understanding of this essential barrier*. Proceedings of the American Thoracic Society **2004**, Vol. 1, Issue 1, *Pages 54-61*.

Van Klinken, B. J.; Dekker, J.; Buller, H. A.; Einerhand, A. W., *Mucin gene structure and expression: protection vs. adhesion*. American Journal of Physiology-Gastrointestinal and Liver Physiology **1995**, Vol. 269, Issue 5, *Pages G613-G627*.

Våset, F. S., *Biosimilar Mucus as a Model System for Small Intestinal Mucus*. **2014.**

Wong, T. W., *Design of oral insulin delivery systems*. Journal of drug targeting **2010**, Vol. 18, Issue 2, *Pages 79-92*.

Woodley, J., *Bioadhesion: New possibilities for drug administration?* Clinical Pharmacokinetics **2001**, Vol. 40, Issue 2, *Pages 77-84*.

Yang, X.; Forier, K.; Steukers, L.; Van Vlierberghe, S.; Dubruel, P.; Braeckmans, K.; Glorieux, S.; Nauwynck, H. J., *Immobilization of Pseudorabies Virus in Porcine Tracheal Respiratory Mucus Revealed by Single Particle Tracking*. PLoS ONE **2012**, Vol. 7, Issue 12.

Yoncheva, K.; Gómez, S.; Campanero, M. A.; Gamazo, C.; Irache, J. M., *Bioadhesive properties of pegylated nanoparticles*. Expert opinion on drug delivery, **2005,** Vol. 2, Issue 2, *Pages 205-218*.

Zhang, F.; Liu, M.; Wan, H., *Discussion about Several Potential Drawbacks of PEGylated Therapeutic Proteins.* Biological and Pharmaceutical Bulletin **2014,** Vol. 37, No. 3, *Pages 335-339*.

# Appendix A: Protocol for PEGylation of carboxylate modified FluoSpheres

This protocol was adapted from Suh *et al.* 2007.

Products:

The following products are used for the PEGylation of the FluoSpheres:

- Carboxylate modified Fluospheres of the desired size and fluorescent spectrum (this protocol is written for a solution containing 2 % solids). Yellow-green, 200 nm (Invitrogen).
- 1-ethyl-3-(3-dimethylaminopropyl)carbodiimide hydrochloride (EDC) (Fluka)
- N-hydroxysulfosuccinimide (Sulfo-NHS) (Aldrich)
- Methoxy-polyethylene glycol-amine (mPEGa), 2000 Daltons (Creative PEGWorks)
- HBS buffer at pH 8 containing: 10 mM HEPES, 150 mM NaCl, 3.4 mM EDTA, 0.005 m% Tween 20

Protocol:

Functionalization:

1. Sonicate the FluoSpheres for 10 minutes prior to use.

2. 4 mg EDC, 1.13 mg Sulfo-NHS and 10 mg mPEGa were dissolved in 0.5 mL HBS.

3. Add 0.5 ml of the Fluospheres to this mixture.

4. Shake overnight at 200 RPM, protected from light and at room temperature.

Purification:

1. Centrifuge the reaction mixture over a centrifugal filter (Amikon ultra, centrifugal filters, 100K membrane, Millipore) for 12 minutes at 12000 RPM.

2. Fill up the filter with 0.5 ml HBS and centrifuge again to wash the FluoSpheres (twice) (12 minutes, 12000 RPM).

3. Collect the FluoSpheres by placing the filter upside down in a new vial followed by centrifugation at 2600 RPM for 10 minutes. Add 50 µL of HBS buffer to the filter. Repeat as long as too many beads remain on the filter.

4. Adjust the volume with HBS to give a final concentration of FluoSpheres of ~ 2 % solids (total volume of 0.5 mL.

5. Make a dilution of the FluoSphere solution 1:100 in HEPES buffer (pH 7.3). Measure the zeta-potential and the bead size using the Zetaziser Nano-ZS (Malvern).

# Appendix B: Method for production of biosimilar mucus (10 mL)

This protocol was adapted from Boegh *et al.* 2013.

1. 100 mL 10 mM isotonic HEPES buffer was produced containing 1.3 mM $CaCl_2$, 1 mM $MgSO_4$ and 137 mM NaCl. 0.2383 g HEPES, 0.01911 g $CaCl_2 \times 2H_2O$, 0.02465 g $MgSO_4 \times 7H_2O$ and 0.80063 g NaCl was weighed out and mixed with 100 mL MQ water.
2. 100 mL 10 mM non-isotonic HEPES buffer was produced containing 1.3 mM $CaCl_2$ and 1 mM $MgSO_4$. 0.2383 g HEPES, 0.01911 g $CaCl_2 \times 2H_2O$ and 0.02465 g $MgSO_4 \times 7H_2O$ was weighed out and mixed with 100 mL MQ water.
3. Lipid solution: 0.0121 g linoleic acid, 0.0396 g cholesterol and 0.033 g phosphatidylcholine was weighed out and mixed in an Eppendorf tube. 0.03586 g polysorbate tween 80 was weighed out and added to the tube, along with two small magnets. 750 µL of isotonic HEPES buffer (10 mM) was added. The tube was left on vigorous magnetic stirring until the solution was visually homogenous.
4. Polymer solution: 0.09 g polyacrylic acid was added to 9.168 mL of non-isotonic HEPES buffer (10 mM) and stirred until dissolved. 0.5 g sigma mucin type II was added and stirred until dissolved. 150 µL 5 mM NaOH was added and the mixture was stirred until homogenous.
5. 0.682 mL of the homogenous lipid solution was added, and the mixture was stirred. 0.31 g bovine albumin was added and the mixture was stirred until homogenous.
6. The pH was adjusted from 4.1 to 7.4 with 1 M NaOH and a pH-meter.
7. The biosimilar mucus was stored cold (ca 3.5 °C) or frozen (ca -20 °C).

# Appendix C: Overview of the setup of all the experiments performed

An overview of all the performed experiments with information about type of nanoparticle, type of mucus, and whether the particles were diluted in G-block solutions or in physiological saline (NaCl), can be found in Table C.1.

Table C.1: An overview of all the performed experiments. The numbers 1 to 8 refer to the wells on an 8-well plate, in which the experiments were prepared.

| Well | 1 | 2 | 3 | 4 | 5 | 6 | 7 | 8 |
|---|---|---|---|---|---|---|---|---|
| Prep. 29/10 2014, filmed 31/10 2014 | | PSIM<br>200 nm PEGylated FluoSpheres<br>NaCl | Biosimilar mucus<br>200 nm PEGylated FluoSpheres<br>NaCl | | | Biosimilar mucus<br>100 nm aminated FluoSpheres<br>NaCl | Biosimilar mucus<br>200 nm PEGylated FluoSpheres<br>NaCl | |
| Prep. 18/11 2014, filmed 19/11 2014 | | Biosimilar mucus<br>200 nm PEGylated FluoSpheres<br>NaCl | Biosimilar mucus<br>100 nm aminated FluoSpheres<br>NaCl | | | PSIM<br>200 nm PEGylated FluoSpheres<br>NaCl | PSIM<br>100 nm aminated FluoSpheres<br>NaCl | |
| Prep. 24/11 2014, filmed 25/11 2014 | Biosimilar mucus<br>200 nm PEGylated FluoSpheres<br>1.0 G-block | Biosimilar mucus<br>200 nm PEGylated FluoSpheres<br>0.1 G-block | Biosimilar mucus<br>200 nm PEGylated FluoSpheres<br>0.01 G-block | Biosimilar mucus<br>200 nm PEGylated FluoSpheres<br>NaCl | Biosimilar mucus<br>100 nm aminated FluoSpheres<br>1.0 G-block | Biosimilar mucus<br>100 nm aminated FluoSpheres<br>0.1 G-block | Biosimilar mucus<br>100 nm aminated FluoSpheres<br>0.01 G-block | Biosimilar mucus<br>100 nm aminated FluoSpheres<br>NaCl |
| Prep. 26/11 2014, filmed 27/11 2014 | PSIM<br>200 nm PEGylated FluoSpheres<br>1.0 G-block | PSIM<br>200 nm PEGylated FluoSpheres<br>0.1 G-block | PSIM<br>200 nm PEGylated FluoSpheres<br>0.01 G-block | PSIM<br>200 nm PEGylated FluoSpheres<br>NaCl | PSIM<br>100 nm aminated FluoSpheres<br>1.0 G-block | PSIM<br>100 nm aminated FluoSpheres<br>0.1 G-block | PSIM<br>100 nm aminated FluoSpheres<br>0.01 G-block | PSIM<br>100 nm aminated FluoSpheres<br>NaCl |
| Prep. 13/01 2015, filmed 14/01 2015 | PSIM<br>200 nm PEGylated FluoSpheres<br>NaCl | PSIM<br>200 nm PEGylated FluoSpheres<br>0.01 G-block | PSIM<br>200 nm PEGylated FluoSpheres<br>0.1 G-block | PSIM<br>200 nm PEGylated FluoSpheres<br>1.0 G-block | PSIM<br>200 nm aminated FluoSpheres<br>NaCl | PSIM<br>200 nm aminated FluoSpheres<br>0.01 G-block | PSIM<br>100 nm aminated FluoSpheres<br>0.1 G-block | PSIM<br>200 nm aminated FluoSpheres<br>1.0 G-block |
| Prep. 02/02 2015, filmed 03/02 2015 | | PSIM<br>200 nm aminated FluoSpheres<br>NaCl | PSIM<br>200 nm aminated FluoSpheres<br>0.01 G-block | | | PSIM<br>200 nm aminated FluoSpheres<br>0.1 G-block | PSIM<br>200 nm aminated FluoSpheres<br>1.0 G-block | |
| Prep. 03/02 2015, filmed 04/02 2015 | | PSIM<br>100 nm carboxylated FluoSpheres<br>NaCl | PSIM<br>100 nm carboxylated FluoSpheres<br>0.01 G-block | | | PSIM<br>100 nm carboxylated FluoSpheres<br>0.1 G-block | PSIM<br>100 nm carboxylated FluoSpheres<br>1.0 G-block | |
| Prep. 04/02 2015, filmed 05/02 2015 | | PSIM<br>200 nm carboxylated FluoSpheres<br>NaCl | PSIM<br>200 nm carboxylated FluoSpheres<br>0.01 G-block | | | PSIM<br>200 nm carboxylated FluoSpheres<br>0.1 G-block | PSIM<br>200 nm carboxylated FluoSpheres<br>1.0 G-block | |
| Prep. 24/02 2015, filmed 25/02 2015 | | Biosimilar mucus<br>100 nm carboxylated FluoSpheres<br>NaCl | Biosimilar mucus<br>200 nm carboxylated FluoSpheres<br>NaCl | | | Biosimilar mucus<br>200 nm aminated FluoSpheres<br>NaCl | | |

## Appendix D: Matlab script for MSD determination

The Matlab script was created by Astrid Bjørkøy in 2011 in order to translate x- and y- coordinates from ImageJ processing on particles tracked with CLSM Leica SP5 into mean-square displacement (MSD) values. The Matlab code is given below.

```
function mpt;
% Prompt for lag time between frames
% Prompt for name of resultfile!
prompt = {'Enter time interval:;\','Enter name of result file:'};
dlg_title = 'Input for Trajectory Calculations';
num_lines = 1;
def = {'time interval','results.txt'};
answer = inputdlg(prompt,dlg_title,num_lines,def);

timeinterval = str2double(answer{1});
filnavn = answer{2};

%Open the file with trajectory data
[File, Path] = uigetfile('*.txt','Open Trajectory file',
'C:\Users\','MultiSelect','Off')

s1 = char(strcat(Path,File));
fid = fopen(s1);

k = 1;
% Figure out what trajectories are in this file, put the names in
% Nr.Trajectory and the number of frames for particle K in Particles
while 1
 tline = fgetl(fid);
 if ~ischar(tline), break, end
 if ~isempty(tline)
   if tline(1) == '%'
       nr = 0;
       Nr(k).Trajectory = tline(4:end);
       k = k+1;
   else nr = nr+1;
   end
 else Particles(k-1) = nr;
 end
end
  fclose(fid);

%Import the trajectory data and put data in newData 1
rawData1 = importdata(s1);

%For some simple files (such as a CSV or JPEG files), IMPORTDATA
might
%return a simple array. If so, generate a structure so that the
output
%matches that form the Import Wizard.
[unused,name] = fileparts(s1);
newData1 = squeeze(rawData1);

%Create new variables in the base workspace from those firlds.
 vars = fieldnames(newData1);
```

```
for i = 1:length(vars)
  assignin('base', vars{i}, newData1.(vars{i}));
end

j = 1;
pend = 0;
%For each particle, calculate the msd's for each time step!
%The frame number and (x,y) for each particle are between pstart and
pend
% in the data file newData 1.
for particle = 1:length(Particles)
  pstart = pend + 1;
  pend = pstart + (Particles(particle)-1);
  % p is an array containing the frame numbers
  p = newData1.data(pstart:pend,1);
  x = newData1.data(pstart:pend,2);
  y = newData1.data(pstart:pend,3);
  % maxstep is the maximum lag time possible for the particle
  maxstep = p(end)-p(1);
  for step = 1:maxstep
    ave = []; % vector of msd's
    i = p(1); % number of startframe
    while i+step <= p(end)
     % ignore frames missing!
     if~ismember(i,p) ||~ismember((i+step),p)
     else
       % find the correct position in p, x and y for i and i+step
       i1 = find(p==i);
       i2 = find(p==(i+step));
       new =((x(i1)-x(i2))^2 + (y(i1)-y(i2))^2);
       ave = [new ave];
     end
     i = i+1;
   end
   if~isempty(ave)
     msd(particle, step)= mean(ave); %mean msd for this step/lag
time
   end
  end
  ost = ['partikkel ', num2str(particle), ' ferdig'];
  disp(ost);
end


% Save the data to a file: lag time in first column, data for the
%particles in the other columns.
datafile = strcat(Path, filnavn);
fid = fopen(char(datafile),'a');

fprintf(fid,'%s','Step');
for i = 1:length(Particles)
  fprintf(fid,'\t%s',Nr(i).Trajectory);
end
fprintf(fid,'\n');

%size(msd,2) is the maximum number of frames for the particles
```

```
% in the data file newData1
for i= 1:size(msd,2)
  fprintf(fid,'%6.4f\t', i*timeinterval);
  for j = 1:length(Particles)
     % if there's data missing for this lag time, skip info!
     % else save the result
     if msd(j,i) == 0 fprintf(fid,'\t');
     else fprintf(fid,'%6.4f\t',msd(j,i));
     end
   end
 fprintf(fid,'\n');
end
```

# Appendix E: Zeta potential measurements

The zeta potential and the bead size of a 1:100 dilution of the PEGylated FluoSphere solution in HEPES buffer (pH 7.3) was measured using a Zetasizer Nano-ZS (Malvern). The results are given in Table E.1 below.

Table E.1: Measurement of size and zeta potential for the PEGylated particles.

| **Size measurement** | | **Zeta potential measurement** | |
|---|---|---|---|
| Sample | Z-Ave d.nm | Sample | ZP mV |
| 11 | 291.5 | 6 | -11 |
| 12 | 287.8 | 7 | -10.6 |
| 13 | 285.9 | 8 | -10.7 |
| 14 | 288.4 | 9 | -10.5 |
| 15 | 288.8 | 10 | -11.8 |
| | | | |
| Std Dev 11-15 | 2.022 | Std Dev 6-10 | 0.526 |
| RSD % | 0.701 | RSD % | 4.82 |
| Average | 288.48 | Average | -10.92 |